WCAP-12020

ANALYSIS OF CAPSULE P FROM THE WISCONSIN PUBLIC SERVICE CORPORATION KEWAUNEE NUCLEAR PLANT REACTOR VESSEL RADIATION SURVEILLANCE PROGRAM

S. E. Yanichko
S. L. Anderson
L. Albertin

November 1988

Work performed under Shop Order No. KYFJ-106

APPROVED: T. A. Meyer
T. A. Meyer, Manager
Structural Materials and Reliability Technology

Prepared by Westinghouse for the Wisconsin Public Service Corporation

WESTINGHOUSE ELECTRIC CORPORATION
Nuclear Advanced Technology Division
P.O. Box 2728
Pittsburgh, Pennsylvania 15230

PREFACE

This report has been technically reviewed and verified.

	Reviewer
Sections 1 through 5, 7 and 8	N. K. Ray
Section 6	E. P. Lippincott

TABLE OF CONTENTS

LIST OF ILLUSTRATIONS

LIST OF ILLUSTRATIONS (Cont)

LIST OF TABLES

LIST OF TABLES (Cont)

LIST OF TABLES (Cont)

SECTION 1
SUMMARY OF RESULTS

The analysis of the reactor vessel material contained in Capsule P, the third surveillance capsule to be removed from the Wisconsin Public Service Corporation Kewaunee reactor pressure vessel, led to the following conclusions:

- The capsule received an average fast neutron fluence (E > 1.0 MeV) of 2.89×10^{19} n/cm^2.

- Irradiation of Charpy V-notch impact specimens from the reactor vessel intermediate shell forging 122X208 VA1, to 2.89×10^{19} n/cm^2, resulted in 30 and 50 ft-lb transition temperature increases of 25°F and 10°F respectively, for specimens oriented parallel to the major working direction (tangential orientation). Irradiation of Charpy V-Notch Impact specimens from the vessel lower shell forging 123X167 VA1 resulted in 30 and 50 ft-lb transition temperature increases of 20°F for tangentially oriented specimens.

- Weld metal impact specimens irradiated to 2.89×10^{19} n/cm^2 resulted in 30 and 50 ft-lb transition temperature increases of 230°F and 235°F respectively.

- Irradiation to 2.89×10^{19} n/cm^2 resulted in a 3 ft-lb decrease in the average upper shelf energy of forging 122X208 VA1 and no decrease in the upper shelf energy of forging 123X167 VA1. The weld metal decreased by 50 ft-lb from 126 to 76 ft-lbs. All materials tested exhibit a more than adequate shelf energy level for continued safe plant operation.

- Comparison of the 30 ft-lb transition temperature increases for the Kewaunee surveillance material with predicted increases using the methods of NRC Regulatory Guide 1.99, Revision 2, shows that the forging material and weld metal transition temperature increase were less than predicted.

SECTION 2
INTRODUCTION

This report presents the results of the examination of Capsule P, the third capsule to be removed from the reactor in the continuing surveillance program which monitors the effects of neutron irradiation on the Kewaunee reactor pressure vessel materials under actual operating conditions.

The surveillance program for the Kewaunee reactor pressure vessel materials was designed and recommended by the Westinghouse Electric Corporation. A description of the surveillance program and the preirradiation mechanical properties of the reactor vessel materials are presented by Yanichko. [1] The surveillance program was planned to cover the 40-year design life of the reactor pressure vessel and was based on ASTM E-185-70, "Recommended Practice for Surveillance Tests on Nuclear Reactors Vessels". Westinghouse Energy Systems personnel were contracted to aid in the preparation of procedures for removing the capsule from the reactor and its shipment to the Westinghouse Research and Development Laboratory, where the postirradiation mechanical testing of the Charpy V-notch impact and tensile surveillance specimens was performed.

This report summarizes testing and the postirradiation data obtained from surveillance Capsule P removed from the Kewaunee reactor vessel and discusses the analysis of the data. The data are also compared to results of the previously removed Kewaunee surveillance Capsule V [2] and Capsule R [3].

SECTION 3
BACKGROUND

The ability of the large steel pressure vessel containing the reactor core and its primary coolant to resist fracture constitutes an important factor in ensuring safety in the nuclear industry. The beltline region of the reactor pressure vessel is the most critical region of the vessel because it is subjected to significant fast neutron exposure. The overall effects of fast neutron irradiation on the mechanical properties of low alloy ferritic pressure vessel steels such as SA 508 Class 2 (base material of the Kewaunee reactor pressure vessel beltline) are well documented in the literature. Generally, low alloy ferritic materials show an increase in hardness and tensile properties and a decrease in ductility and toughness under certain conditions of irradiation.

A method for performing analyses to guard against fast fracture in reactor pressure vessels has been presented in "Protection Against Non-ductile Failure," Appendix G to Section III of the ASME Boiler and Pressure Vessel Code. The method utilizes fracture mechanics concepts and is based on the reference nil-ductility temperature (RT_{NDT}).

RT_{NDT} is defined as the greater of either the drop weight nil-ductility transition temperature (NDTT per ASTM E-208) or the temperature 60°F less than the 50 ft lb (and 35-mil lateral expansion) temperature as determined from Charpy specimens oriented normal (transverse) to the major working direction of the material. The RT_{NDT} of a given material is used to index that material to a reference stress intensity factor curve (K_{IR} curve) which appears in Appendix G of the ASME Code. The K_{IR} curve is a lower bound of dynamic, crack arrest, and static fracture toughness results obtained from several heats of pressure vessel steel. When a given material is indexed to the K_{IR} curve, allowable stress intensity factors can be obtained for this material as a function of temperature. Allowable operating limits can then be determined utilizing these allowable stress intensity factors.

RT_{NDT} and, in turn, the operating limits of nuclear power plants can be adjusted to account for the effects of radiation on the reactor vessel material properties. The radiation embrittlement or changes in mechanical properties of a given reactor pressure vessel steel can be monitored by a reactor surveillance program such as the Kewaunee Reactor Vessel Radiation Surveillance Program, [1] in which a surveillance capsule is periodically removed from the operating nuclear reactor and the encapsulated specimens are tested. The increase in the average Charpy V-notch 30 ft lb temperature (ΔRT_{NDT}) due to irradiation is added to the original RT_{NDT} to adjust the RT_{NDT} for radiation embrittlement. This adjusted RT_{NDT} (RT_{NDT} initial + ΔRT_{NDT}) is used to index the material to the K_{IR} curve and, in turn, to set operating limits for the nuclear power plant which take into account the effects of irradiation on the reactor vessel materials.

The unirradiated fracture toughness properties of the Kewaunee reactor vessel material are identified in table 3-1.

TABLE 3-1
REACTOR VESSEL TOUGHNESS DATA (UNIRRADIATED)

COMPONENT	CODE NO.	MATERIAL GRADE	Cu (%)	P (%)	Ni (%)	NDTT (°F)	RT_{NDT} (°F)	NMWD UPPER SHELF ENERGY (FT LB)
Closure head dome	B6301	A533B Cl. 1	-	0.010	0.58	0	0	75[a]
Closure Head flange	B6302	A508 Cl. 2	0.16	0.011	0.76	60[a]	60	76[a]
Vessel flange	B6303	A508 Cl. 2	0.14	0.010	0.68	60[a]	60	86.5[a]
Injection nozzle	B6310-1	A508 Cl. 2	-	0.004	0.71	60[a]	60	74[a]
Injection nozzle	B6310-2	A508 Cl. 2	-	0.004	0.71	60[a]	60	65.5[a]
Inlet nozzle	B6309-1	A508 Cl. 2	-	0.010	0.68	48[a]	48	89[a]
Inlet nozzle	B6309-2	A508 Cl. 2	-	0.010	0.76	60[a]	60	86[a]
Outlet nozzle	B6308-1	A508 Cl. 2	-	0.010	0.83	60[a]	60	88.5[a]
Outlet nozzle	B6308-2	A508 Cl. 2	-	0.010	0.72	26[a]	26	108.5[a]
Nozzle Shell	B6305	A508 Cl. 2	-	0.010	0.70	40	40	85.5[a]
Intermediate shell	B6306	A508 Cl. 2	0.06	0.010	0.71	60	60	141.5[a]
Lower shell	B6307	A508 Cl. 2	0.06	0.010	0.75	20	20	149
Bottom Head Ring	B6312	A508 Cl. 2	-	0.011	0.73	-10	10	85[a]
Bottom Head Dome	B6313	A533B Cl. 1	0.11	0.015	0.55	-30	-30	100.5[a]
Inter to Lower Shell Weld (B4 Mod. Wire IP3571 + Linde 1092)			0.20	0.016	0.77	0[a]	-56(c)	126

(a) Estimated using methods identified in NRC Standard Review Plan section 5.3.2 pressure temperature limits.

(b) NMWD = Normal to Major Working Direction.

(c) Generic mean value estimated per 10CFR 50.61 PTS rule.

3342s/012498:10

SECTION 4
DESCRIPTION OF PROGRAM

Six surveillance capsules for monitoring the effects of neutron exposure on the Kewaunee reactor pressure vessel core region material were inserted in the reactor vessel prior to initial plant startup. The capsules were positioned in the reactor vessel between the neutron shield pads and the vessel wall at locations shown in figure 4-1. The vertical center of the capsules is opposite the vertical center of the core.

Capsule P (Figure 4-2) was removed after 11.08 effective full power years of plant operation. This capsule contained Charpy V-notch impact, tensile, and 1X Wedge Opening Loading (WOL) fracture mechanics specimens from the reactor vessel intermediate shell ring forging 122X208 VA1 and lower shell ring forging 123X167 VA1, and Charpy V-notch specimens from submerged arc weld metal identical to the beltline region girth weld seam of the reactor vessel and weld heat-affected zone (HAZ) material. All heat-affected zone specimens were obtained from within the HAZ of forging 122X208 VA1. The capsule also contained Charpy V-notch specimens from the 12-inch thick ASTM correlation monitor material (HSST plate 02).

The chemistry and heat treatment of the surveillance material are presented in table 4-1 and 4-2. The chemical analyses reported in table 4-1 were obtained from unirradiated material used in the surveillance program.

All test specimens were machined from the 1/4 thickness location of the forgings. Test specimens represent material taken at least one forgings thickness from the quenched end of the forgings. All base metal Charpy V-notch impact and tensile specimens were oriented with the longitudinal axis of the specimen parallel to (tangential orientation) the principal working direction of the forgings. Charpy V-notch specimens from the weld metal were oriented with the longitudinal axis of the specimens transverse to the weld direction. The Wedge Opening Loading (WOL) test specimens in Capsule P were machined parallel to the major working direction (tangential orientation). All specimens were fatigue precracked per ASTM E399-70T.

Capsule P contained dosimeter wires of pure iron, copper, nickel, and unshielded aluminum-cobalt. In addition, cadmium-shielded dosimeters of Neptunium (Np^{237}) and Uranium (U^{238}) were contained in the capsule.

Thermal monitors made from two low-melting eutectic alloys and sealed in Pyrex tubes were included in the capsule and were located as shown in figure 4-2. The two eutectic alloys and their melting points are:

2.5% Ag, 97.5% Pb	Melting Point 579°F (304°C)
1.75% Ag, 0.75% Sn, 97.5% Pb	Melting Point 590°F (310°C)

The arrangement of the various mechanical test specimens, dosimeters and thermal monitors contained in Capsule P are shown in figure 4-2.

TABLE 4-1

CHEMICAL COMPOSITION AND HEAT TREATMENT OF THE KEWAUNEE REACTOR VESSEL SURVEILLANCE MATERIALS

	CHEMICAL ANALYSIS (wt %)		
Element	Forging 122X208VA1	Forging 123X167VA1	Weld Metal
C	0.21	0.20	0.12
Si	0.25	0.28	0.20
Mo	0.58	0.58	0.48
Cu	0.06	0.06	0.20
Ni	0.71	0.75	0.77
Mn	0.69	0.79	1.37
Cr	0.40	0.35	0.090
V	<0.02	<0.02	0.002
Co	0.011	0.012	0.001
Sn	0.01	0.01	0.004
Ti	<0.001	<0.001	<0.001
Zr	0.001	0.001	<0.001
As	0.001	0.004	0.004
Sb	<0.001	0.00[illegible]	0.001
S	0.011	0.00[illegible]	0.011
P	0.010	0.010	0.016
Al	0.004	0.005	0.010
B	<0.003	<0.003	<0.003
N_2	0.006	0.010	0.012
Zn	-	-	<0.001

HEAT TREATMENT

Intermediate Shell Forging Heat 122X208VA1	Heated at 1550°F for 8 hours, water quenched Tempered at 1230°F for 14 hours, air-cooled Stress-relieved at 1150°F for 21 hours, furnace-cooled
Lower Shell Forging Heat 123X167VA1	Heated at 1550°F for 8 hours, water-quenched Tempered at 1220°F for 14 hours, air-cooled Stress-relieved at 1150°F for 21 hours, furnace-cooled
Submerged Arc Weldment	Stress-relieved at 1150°F for 19-1/4 hours, furnace-cooled

---

The weldment was fabricated by Combustion Engineering, Inc., using 3/16 inch Mil B-4 modified weld filler wire, heat number I[illegible]71 and Linde 1092 flux, lot number 3958 and is identical to that used in the actual fabrication of the reactor vessel intermediate to lower shell girth weld seam.

TABLE 4-2

CHEMISTRY AND HEAT TREATMENT OF A533 GRADE B CLASS 1
ASTM CORRELATION MONITOR MATERIAL (HSST PLATE 02)

Chemical Analysis (wt%)

C	Mn	P	S	Si	Ni	Mo	Cu
0.22	1.48	0.012	0.018	0.25	0.68	0.52	0.14

Heat Treatment

Heated at 1675 ± 25°F - 4 hours - air cooled
Heated at 1600 ± 25°F - 4 hours - water-quenched
Tempered at 1225 ± 25°F - 4 hours - furnace-cooled
Stress-relieved at 1150 ± 25°F - 40 hours - furnace-cooled to 600°F

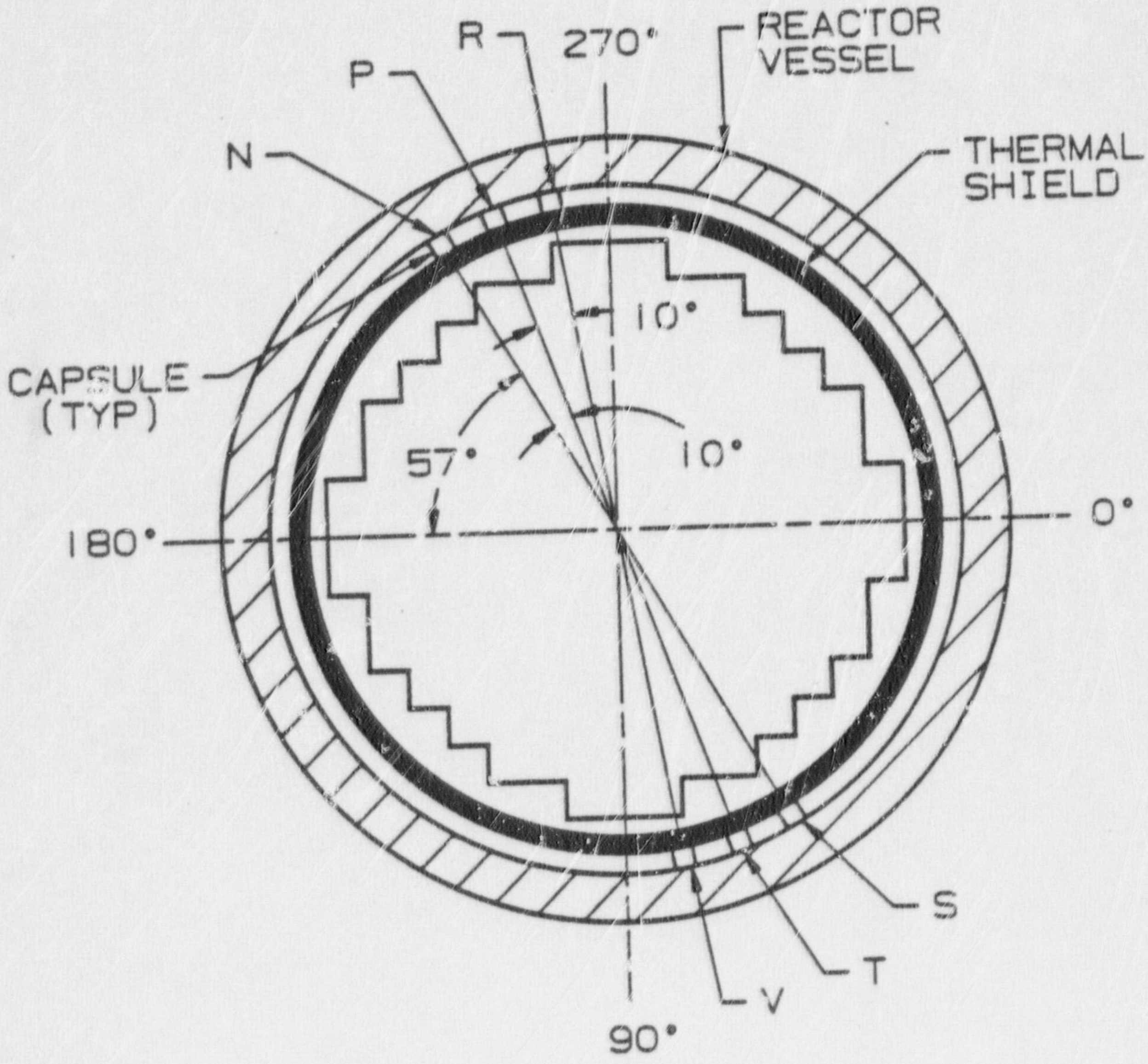

Figure 4-1. Arrangement of surveillance capsules in the reactor vessel

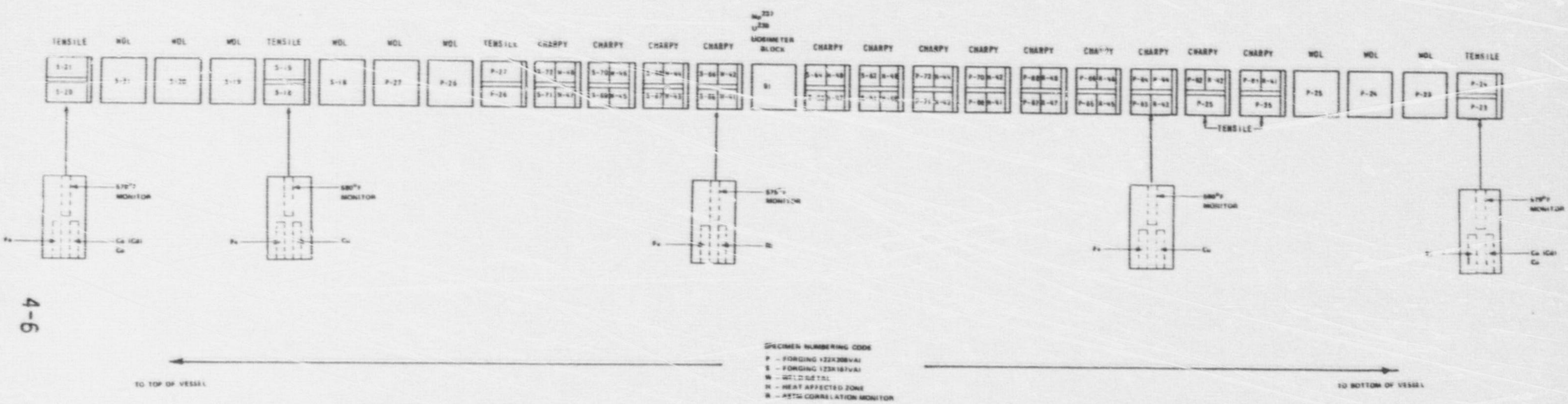

Figure 4-2. Capsule P Diagram Showing Location of Specimens, Thermal Monitors, and Dosimeters

SECTION 5
TESTING OF SPECIMENS FROM CAPSULE P

5-1. OVERVIEW

The postirradiation mechanical testing of the Charpy V-notch and tensile specimens was performed at the Westinghouse Research and Development Laboratory with consultation by Westinghouse Energy Systems personnel. Testing was performed in accordance with 10CFR50, Appendices G and H[4], ASTM Specification E185-82 and Westinghouse Procedure MHL 8402, Revision 0 as modified by RMF Procedures 8102 and 8103.

Upon receipt of the capsule at the laboratory, the specimens and spacer blocks were carefully removed, inspected for identification number, and checked against the master list in WCAP-8908 [1]. No discrepancies were found.

Examination of the two low-melting 304°C (579°F) and 310°C (590°F) eutectic alloys indicated no melting of either type of thermal monitor. Based on this examination, the maximum temperature to which the test specimens were exposed was less than 304°C (579°F).

The Charpy impact tests were performed per ASTM Specification E23-82 and RMF Procedure 8103 on a Tinius-Olsen Model 74, 358J machine. The tup (striker) of the Charpy machine is instrumented with an Effects Technology model 500 instrumentation system. With this system, load-time and energy-time signals can be recorded in addition to the standard measurement of Charpy energy (E_D). From the load-time curve, the load of general yielding (P_{GY}), the time to general yielding (t_{GY}), the maximum load (P_M), and the time to maximum load (t_M) can be determined. Under some test conditions, a sharp drop in load indicative of fast fracture was observed. The load at which fast fracture was initiated is identified as the fast fracture load (P_F), and the load at which fast fracture terminated is identified as the arrest load (P_A).

The energy at maximum load (E_M) was determined by comparing the energy-time record and the load-time record. The energy at maximum load is approximately equivalent to the energy required to initiate a crack in the specimen. Therefore, the propagation energy for the crack (E_p) is the difference between the total energy to fracture (E_D) and the energy at maximum load.

The yield stress (σ_y) is calculated from the three point bend formula. The flow stress is calculated from the average of the yield and maximum loads, also using the three point bend formula.

Percentage shear was determined from postfracture photographs using the ratio-of-areas methods in compliance with ASTM Specification A370-77. The lateral expansion was measured using a dial gage rig similar to that shown in the same specification.

Tension tests were performed on a 20,000-pound Instron, split-console test machine (Model 1115) per ASTM Specifications E8-83 and E21-79, and RMF Procedure 8102. All pull rods, grips, and pins were made of Inconel 718 hardened to Rc45. The upper pull rod was connected through a universal joint to improve axiality of loading. The tests were conducted at a constant crosshead speed of 0.05 inch per minute throughout the test.

Deflection measurements were made with a linear variable displacement transducer (LVDT) extensometer. The extensometer knife edges were spring-loaded to the specimen and operated through specimen failure. The extensometer gage length is 1.00 inch. The extensometer is rated as Class B-2 per ASTM E83-67.

Elevated test temperatures were obtained with a three-zone electric resistance split-tube furnace with a 9-inch hot zone. All tests were conducted in air.

Because of the difficulty in remotely attaching a thermocouple directly to the specimen, the following procedure was used to monitor specimen temperature. Chromel-alumel thermocouples were inserted in shallow holes in the center and each end of the gage section of a dummy specimen and in each grip. In the test configuration, with a slight load on the specimen, a plot of specimen temperature versus upper and lower grip and controller temperatures was developed over the range room temperature to 550°F (288°C). The upper grip was used to control the furnace temperature. During the actual testing the grip temperatures were used to obtain desired specimen temperatures. Experiments indicated that this method is accurate to plus or minus 2°F.

The yield load, ultimate load, fracture load, total elongation, and uniform elongation were determined directly from the load-extension curve. The yield strength, ultimate strength, and fracture strength were calculated using the original cross-sectional area. The final diameter and final gage length were determined from postfracture photographs. The fracture area used to calculate the fracture stress (true stress at fracture) and percent reduction in area was computed using the final diameter measurement.

5.2. CHARPY V-NOTCH IMPACT TEST RESULTS

The results of Charpy V-notch impact tests performed on the various materials contained in Capsule P irradiated to approximately 550°F at 2.89×10^{19} n/cm^2 are presented in tables 5-1 through 5-6 and figures 5-1 through 5-5. The transition temperature increases and upper shelf energy decreases for the Capsule P material are shown in table 5-7.

Irradiation of the vessel intermediate shell forging 122X208 VA1 material (tangential orientation) specimens to 2.89×10^{19} n/cm^2 (figure 5-1) resulted in 30 and 50 ft-lb transition temperature increases of 25°F and 10°F respectively, and an upper shelf energy decrease of 3 ft-lb when compared to the unirradiated data from reference [1].

Irradiation of the vessel lower shell forging 123X167 VA1 material (tangential orientation) specimens to 2.89 x 10^{19} n/cm^2 (figure 5-2) resulted in both 30 or 50 ft-lb transition temperature increases of 20°F and no upper shelf energy decrease of when compared to the unirradiated data.

Weld metal irradiated to 2.89 x 10^{19} n/cm^2 (figure 5-3) resulted in a 30 and 50 ft-lb transition temperature increase of 230°F and 235°F respectively, and an upper shelf energy decrease of 50 ft-lb from 126 to 76 ft-lbs.

Weld HAZ metal irradiated to 2.89 x 10^{19} n/cm^2 (figure 5-4) resulted in 30 and 50 ft-lb transition temperature increases of 220°F and an upper shelf energy decrease of 44 ft-lb.

ASTM correlation monitor material (HSST Plate j02) irradiated to 2.89 x 10^{19} n/cm^2 (figure 5-5) showed a 30 and 50 ft-lb transition temperature increase of 155°F and an upper shelf decrease of 22 ft-lb. These value are similar to those obtained from other surveillance capsule programs.

The fracture appearance of each irradiated Charpy specimen from the various materials is shown in figures 5-6 through 5-10 and show an increasing ductile or tougher appearance with increasing test temperature.

Table 5-7 shows a comparison of the 30 ft-lb transition temperature (ΔRT_{NDT}) increases for the various Kewaunee surveillance materials with predicted increases using the methods of proposed NRC Regulatory Guide 1.99, Revision 2. [5] This comparison shows that the transition temperature increase resulting from irradiation to 2.89 x 10^{19} n/cm^2 is approximately 25°F less than predicted by the Guide for the shell forgings. The weld metal transition temperature increase resulting from irradiation to 2.89 x 10^{19} n/cm^2 is 12°F less than the Guide prediction.

5-3. TENSION TEST RESULTS

The results of tension tests performed on the shell forgings 122X208 VA1 and 123X167 VA1 (tangential orientation) irradiated to 2.89 x 10^{19} n/cm^2 are shown in table 5-9 and figures 5-11, and 5-12, respectively. These results show that irradiation produced approximately a 10 Ksi increase in 0.2 percent yield strength for the shell forgings. Fractured tension specimens for each of the materials are shown in figures 5-13, and 5-14. A typical stress-strain curve for the tension specimens is shown in figure 5-15.

5-4. WEDGE OPENING LOADING TESTS

Per the surveillance capsule testing contract with the Wisconsin Public Service Corporation, 1X - Wedge Opening Loading fracture mechanics specimens will not be tested and will be stored at the Hot Cell at the Westinghouse R&D Center.

TABLE 5-1

CHARPY V-NOTCH IMPACT DATA FOR THE KEWAUNEE REACTOR VESSEL SHELL FORGINGS IRRADIATED AT 550°F, FLUENCE 2.89 x 10^{19} n/cm^2 (E > 1.0 MeV)

Sample No.	Temperature (°F)	Temperature (°C)	Impact Energy (ft-lb)	Impact Energy (J)	Lateral Expansion (mils)	Lateral Expansion (mm)	Shear (%)
			FORGING 122X208VA1 Tangential Orientation				
P62	- 90	(-68)	5.0	(7.0)	6.5	(0.17)	5
P63	- 50	(-46)	32.0	(43.5)	24.5	(0.62)	20
P64	0	(-18)	20.2	(27.0)	17.5	(0.44)	15
P70	0	(-18)	26.0	(35.5)	20.0	(0.51)	20
P61	25	(- 4)	98.0	(133.0)	77.5	(1.97)	65
P66	50	(10)	18.0	(24.5)	19.5	(0.50)	20
P65	50	(10)	95.0	(129.0)	71.0	(1.80)	85
P71	76	(24)	115.0	(156.0)	77.0	(1.96)	100
P68	125	(52)	153.0	(207.5)	91.5	(2.32)	100
P69	200	(93)	160.0	(217.0)	91.0	(2.31)	100
P67	300	(149)	157.0	(213.0)	95.0	(2.41)	100
P72	MACHINE MALFUNCTION						
			FORGING 123X167VA1 Tangential Orientation				
S70	- 50	(-46)	28.0	(38.0)	21.0	(0.53)	20
S68	- 25	(-32)	30.0	(40.5)	26.0	(0.66)	20
S69	- 25	(-32)	8.0	(11.0)	8.0	(0.20)	5
S63	0	(-18)	77.0	(104.5)	61.0	(1.55)	60
S71	0	(-18)	44.0	(59.5)	42.0	(1.07)	35
S67	25	(- 4)	80.0	(108.5)	64.0	(1.63)	70
S65	50	(10)	95.0	(129.0)	73.0	(1.85)	95
S62	76	(24)	107.0	(145.0)	71.0	(1.80)	100
S66	125	(52)	155.0	(210.0)	92.0	(2.34)	100
S61	200	(93)	159.0	(215.5)	89.0	(2.26)	100
S64	300	(149)	170.0	(230.5)	83.0	(2.11)	100
S72	400	(204)	152.0	(206.0)	82.0	(2.08)	100

TABLE 5-2

CHARPY V-NOTCH IMPACT DATA FOR THE KEWAUNEE
REACTOR VESSEL WELD METAL AND HAZ METAL IRRADIATED AT 550°F
FLUENCE 2.89 x 10^{19} n/cm^2 (E > 1.0 MeV)

Sample No.	Temperature (°F)	(°C)	Impact Energy (ft-lb)	(J)	Lateral Expansion (mils)	(mm)	Shear (%)
			Weld Metal				
W44	100	(38)	6.0	(8.0)	14.0	(0.36)	10
W42	150	(66)	26.0	(35.5)	25.0	(0.64)	25
W46	175	(79)	22.0	(30.0)	24.0	(0.61)	25
W48	200	(93)	37.0	(50.0)	32.0	(0.81)	35
W41	250	(121)	63.0	(85.5)	55.0	(1.40)	60
W43	350	(177)	73.0	(99.0)	60.0	(1.52)	100
W45	400	(204)	73.0	(99.0)	61.0	(1.55)	100
W47	450	(232)	83.0	(113.5)	67.0	(1.70)	100
			HAZ Metal				
H43	0	(-18)	12.0	(16.5)	14.0	(0.36)	10
H44	76	(24)	24.0	(32.5)	19.0	(0.48)	20
H45	150	(66)	133.0	(180.5)	85.0	(2.16)	100
H47	150	(66)	63.0	(85.5)	45.0	(1.14)	60
H41	200	(93)	111.0	(150.5)	82.5	(2.10)	100
H42	250	(121)	103.0	(139.5)	73.0	(1.85)	100
H48	350	(177)	134.0	(181.5)	91.0	(2.31)	100
H46	450	(232)	137.0	(185.5)	83.0	(2.11)	100

TABLE 5-3

CHARPY V-NOTCH IMPACT DATA FOR THE KEWAUNEE ASTM CORRELATION MONITOR MATERIAL IRRADIATED AT 550°F FLUENCE 2.89 x 10^{19} n/cm^2 (E > 1.0 MeV)

Sample No.	Temperature (°F)	(°C)	Impact Energy (ft-lb)	(J)	Lateral Expansion (mils)	(mm)	Shear (%)
R41	100	(38)	9.0	(12.0)	9.0	(0.23)	10
R45	150	(66)	23.0	(31.0)	21.0	(0.53)	20
R46	200	(93)	29.0	(39.5)	24.0	(0.61)	30
R42	200	(93)	25.0	(34.0)	24.0	(0.61)	25
R47	250	(121)	60.0	(81.5)	48.0	(1.22)	65
R44	300	(149)	96.0	(130.0)	79.0	(2.01)	100
R48	350	(177)	108.0	(146.5)	82.0	(2.08)	100
R43	450	(232)	98.0	(133.0)	89.0	(2.26)	100

TABLE 5-4

IRRADIATED INSTRUMENTED CHARPY IMPACT TEST RESULTS FOR KEWAUNEE

REACTOR VESSEL SHELL FORGINGS

Sample Number	Test Temp (°F)	Charpy Energy (ft-lb)	Normalized Energies (ft-lb/in²) Charpy Ed/A	Maximum Em/A	Prop Ep/A	Yield Load (kips)	Time to Yield (μsec)	Maximum Load (kips)	Time to Maximum (μsec)	Fracture Load (kips)	Arrest Load (kips)	Yield Stress (ksi)	Flow Stress (ksi)
						FORGING 122X208VA1							
P62	-90	5.0	40	19	21	2.00	45	3.45	80	3.45	0.20	65	90
P63	-50	32.0	258	140	18	3.60	90	4.74	495	4.75	0.20	118	138
P64	0	20.0	161	139	22	3.25	100	4.35	350	4.35	0.30	107	125
P70	0	26.0	209	223	-14	3.95	80	5.15	425	5.15	0.55	130	150
P61	25	98.0	789	362	427	3.20	85	4.85	730	3.85	-	106	133
P66	50	18.0	145	99	45	3.05	80	4.00	255	3.95	-	102	117
P65	50	95.0	765	343	422	3.05	80	4.60	720	3.65	0.30	100	126
P71	76	115.0	926	340	586	3.55	80	5.05	655	3.40	0.65	118	143
P68	125	153.0	1232	350	872	3.35	80	4.90	715	-	-	110	136
P69	200	160.0	1288	321	968	2.50	80	4.20	760	-	-	82	110
P67	300	157.0	1264	296	968	2.50	90	3.95	730	-	-	83	107
P72	MACHINE MALFUNCTION			-	-	-	-	-	-	-	-	-	-
						FORGING 123X167VA1							
S70	-50	28.0	225	209	17	3.45	90	4.90	430	4.90	0.35	114	138
S69	-25	8.0	64	39	26	3.60	85	3.90	120	3.90	-	120	124
S68	-25	30.0	242	233	8	3.60	80	4.70	480	4.70	-	118	137
S71	0	44.0	354	360	- 6	4.05	80	5.35	645	5.30	0.35	135	156
S63	0	77.0	620	331	289	3.35	85	5.00	650	4.3	-	111	138
S67	25	80.0	644	317	327	3.25	90	4.75	650	4.05	-	108	133
S65	50	95.0	765	357	408	3.75	100	5.30	675	3.90	-	124	150
S62	76	107.0	862	350	512	3.65	80	5.30	650	4.10	0.50	121	148
S66	125	155.0	1248	328	920	3.00	90	4.40	730	-	-	100	122
S61	200	159.0	1280	321	959	3.55	215	4.60	705	-	-	118	135
S64	300	170.0	1369	321	1048	2.45	75	4.10	760	-	-	80	108
S72	400	152.0	1224	295	929	2.60	115	3.95	720	-	-	87	109

TABLE 5-5

IRRADIATED INSTRUMENTED CHARPY IMPACT TEST RESULTS FOR KEWAUNEE

REACTOR VESSEL WELD METAL AND HAZ METAL

Sample Number	Test Temp (°F)	Charpy Energy (ft-lb)	Normalized Energies (ft-lb/in^2) Charpy Ed/A	Maximum Em/A	Prop Ep/A	Yield Load (kips)	Time to Yield (μsec)	Maximum Load (kips)	Time to Maximum (μsec)	Fracture Load (kips)	Arrest Load (kips)	Yield Stress (ksi)	Flow Stress (ksi)
							Weld Metal						
W44	100	6.0	48	33	16	3.45	95	4.00	120	4.00	-	114	123
W42	150	26.0	209	158	51	3.65	90	4.50	345	4.45	0.70	121	135
W46	175	22.0	177	136	42	3.30	85	4.35	310	4.34	0.90	109	127
W48	200	37.0	298	182	116	3.55	120	4.60	375	4.40	1.55	118	135
W41	250	63.0	507	236	271	3.15	90	4.60	505	4.50	3.75	105	128
W43	350	73.0	588	183	405	3.15	105	4.30	435	-	-	104	123
W45	400	73.0	588	220	368	3.05	85	4.20	500	-	-	101	120
W47	450	83.0	1075	219	884	2.9	90	4.25	500	-	-	95	118
							HAZ Metal						
H43	0	12.0	97	85	12	3.90	85	4.45	200	4.40	0.15	130	138
H44	76	24.0	193	173	21	4.00	110	5.30	360	5.15	0.35	133	154
H47	150	63.0	507	278	230	3.35	85	4.70	570	4.25	1.40	110	133
H45	150	133.0	1071	357	714	3.75	100	5.30	675	3.90	-	124	150
H41	200	111.0	894	305	589	2.95	95	4.65	655	-	-	97	126
H42	250	103.0	829	287	542	3.25	175	4.60	620	-	-	107	130
H48	350	134.0	1079	274	805	2.90	125	4.35	620	-	-	96	120
H46	450	137.0	1103	308	795	2.65	85	4.20	705	-	-	89	113

TABLE 5-6

IRRADIATED INSTRUMENTED CHARPY IMPACT TEST RESULTS

FOR KEWAUNEE ASTM CORRELATION MONITOR MATERIAL

Sample Number	Test Temp (°F)	Charpy Energy (ft-lb)	Normalized Energies (ft-lb/in^2) Charpy Ed/A	Maximum Em/A	Prop Ep/A	Yield Load (kips)	Time to Yield (μsec)	Maximum Load (kips)	Time to Maximum (μsec)	Fracture Load (kips)	Arrest Load (kips)	Yield Stress (ksi)	Flow Stress (ksi)
R41	100	9.0	72	42	30	3.55	80	3.80	125	3.80	0.25	114	121
R45	150	23.0	185	160	25	3.60	80	4.80	335	4.80	-	119	139
R42	200	25.0	201	153	43	3.05	80	4.55	355	4.55	1.35	100	125
R46	200	29.0	234	182	51	3.30	80	4.50	400	4.50	0.45	108	128
R47	250	60.0	433	264	219	3.55	80	5.30	495	5.20	3.40	117	146
R44	300	96.0	773	271	502	2.90	80	4.30	605	-	-	97	119
R48	350	108.0	870	309	561	3.65	175	4.95	605	-	-	121	143
R43	450	98.0	789	262	527	2.60	85	4.25	605	-	-	86	113

3342s-101781:10

TABLE 5-7

THE EFFECT OF 550°F IRRADIATION AT 2.89×10^{19} n/cm^2 (E > 1.0 MeV) ON THE NOTCH TOUGHNESS PROPERTIES OF THE KEWAUNEE REACTOR VESSEL MATERIALS

	Average 30 ft-lb Temp (°F)			Average 35 mil Lateral Expansion Temp (°F)			Average 50 ft-lb Temp (°F)			Average Energy Absorption at Full Shear (ft-lb)		
Material	Unirradiated	Irradiated	ΔT	Unirradiated	Irradiated	ΔT	Unirradiated	Irradiated	ΔT	Unirradiated	Irradiated	Δ(ft-lb)
122X208 VA1 (tangential)	-25	0	25	-15	15	30	15	25	10	160	157	-3
123X167 VA1 (tangential)	-50	-30	20	-45	-10	35	-25	-5	20	157	159	+2(a)
Weld Metal	-50	180	230	-35	205	240	-10	225	235	126	76	-50
HAZ Metal	-115	105	220	-100	120	220	-70	150	220	180	136	-44
ASTM Monitor	45	200	155	60	225	165	80	235	155	123	101	-22

(a) Increase in shelf energy

3342s/101988:10

TABLE 5-8

COMPARISON OF KEWAUNEE

REACTOR VESSEL SURVEILLANCE CAPSULE CHARPY IMPACT TEST RESULTS

WITH REGULATORY GUIDE 1.99 REVISION 2 PREDICTIONS

			ΔRT_{NDT} (30 ft-lb Increase)		Δ USE	
Material	Capsule	Fluence $10^{19} n/cm^2$	R.G. 1.99 Rev.2 (°F)	Measured (°F)	R.G. 1.99 Rev. 2 (%)	Measured (%)
Forging 122X208 VA1	V	0.599	32	0	17	0
	R	2.07	44	15	22.5	0
	P	2.89	47	25	24	2
Forging 123X167 VA1	V	0.599	32	0	17	0
	R	2.07	44	20	22.5	2.5
	P	2.89	47	20	24	0
Weld Metal	V	0.599	162	175	30	35
	R	2.07	226	235	40	38
	P	2.89	242	230	44	39.5
HAZ Metal	V	0.599	-	80	-	19.5
	R	2.07	-	150	-	21.5
	P	2.89	-	220	-	24.5
Correlation Monitor	V	0.599	87	95	20	11.5
	R	2.07	122	140	27	23
	P	2.89	131	155	29	18

3342s-120888:10

TABLE 5-9

TENSILE PROPERTIES FOR KEWAUNEE

REACTOR VESSEL MATERIAL IRRADIATED TO 2.89 x 10^{19} n/cm^2 (E > 1.0 MeV)

Material	Sample Number	Test Temp. (°F)	0.2% Yield Strength (ksi)	Ultimate Strength (ksi)	Fracture Load (kip)	Fracture Stress (ksi)	Fracture Strength (ksi)	Uniform Elongation (%)	Total Elongation (%)	Reduction in Area (%)
Forging	P25	50	77.9	97.8	2.85	210.2	58.1	10.5	23.7	72
122X208VA1	P26	78	72.3	91.7	2.80	189.7	57.0	11.3	24.5	70
(Tang.)	P23	150	71.8	91.7	2.67	205.6	54.4	9.8	23.3	74
	P27	300	66.2	85.6	2.63	185.7	53.6	9.5	21.9	71
	P24	550	70.3	95.7	2.88	195.1	58.7	9.0	21.6	70
Forging	S21	25	76.4	97.7	2.79	224.4	56.7	10.8	25.1	75
123X167VA1	S19	75	75.9	94.7	2.80	197.7	57.0	10.5	24.8	71
(Tang.)	S20	300	67.7	87.6	2.63	178.2	53.6	9.0	21.0	70
	S18	550	66.2	89.2	2.86	164.9	58.3	8.9	20.1	65

3342s-101788 10

Curve 756429-A

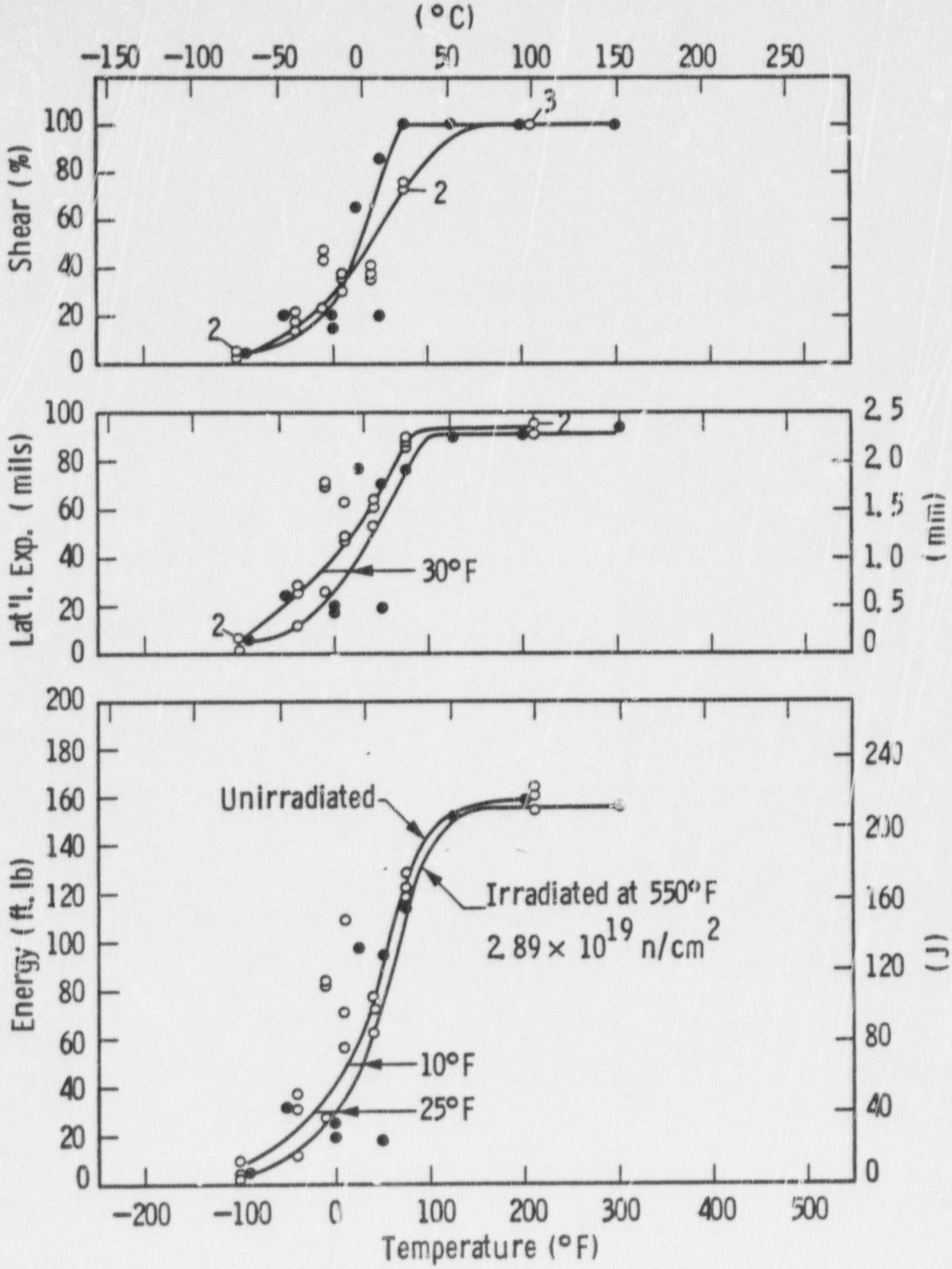

Figure 5-1 Charpy V-notch Impact Properties for Kewaunee Reactor Vessel Shell Forging 122X208 VA1 (Tangential Orientation)

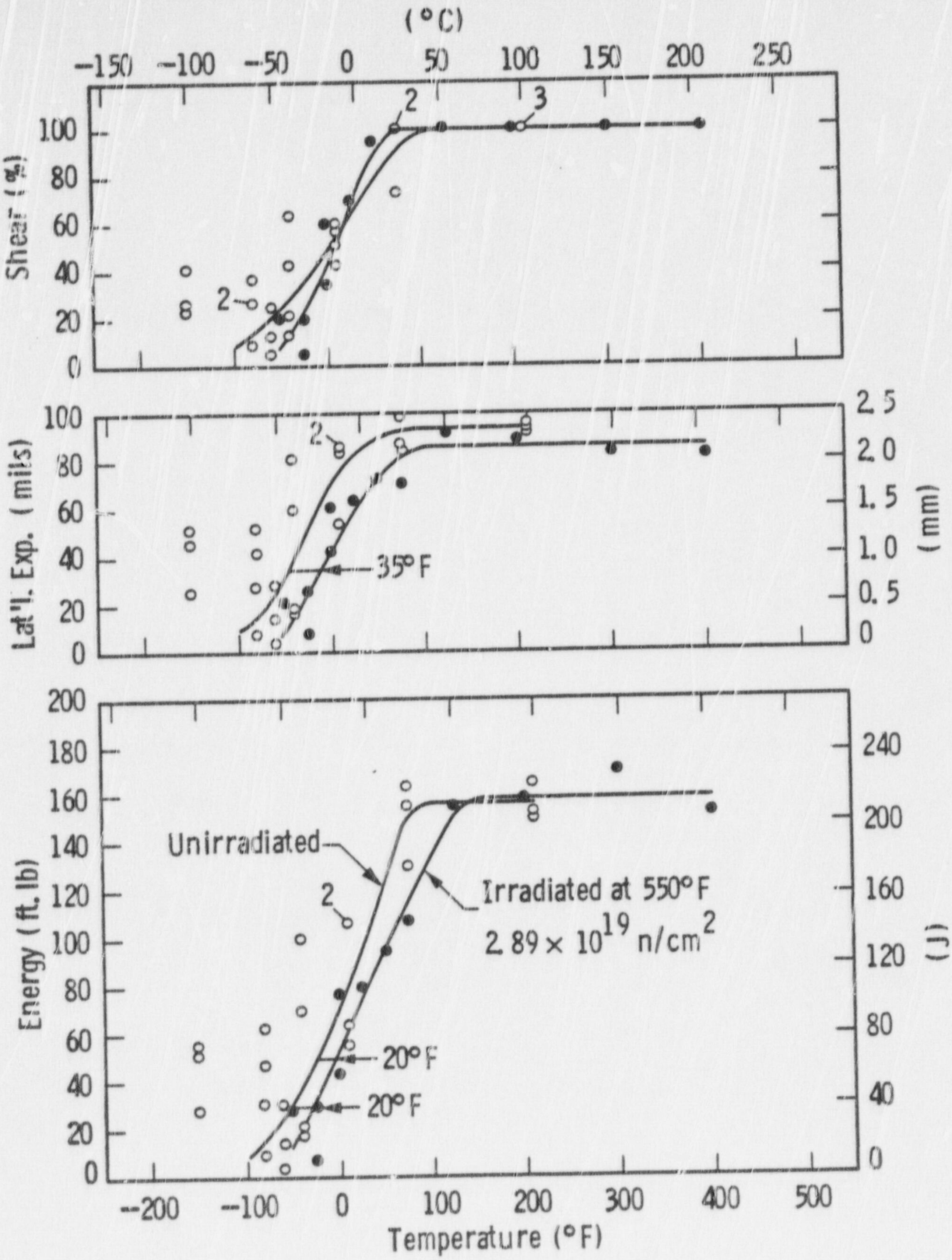

Figure 5-2 Charpy V-notch Impact Properties for Kewaunee Reactor Vessel Shell Forging 123X167 VA1 (Tangential Orientation)

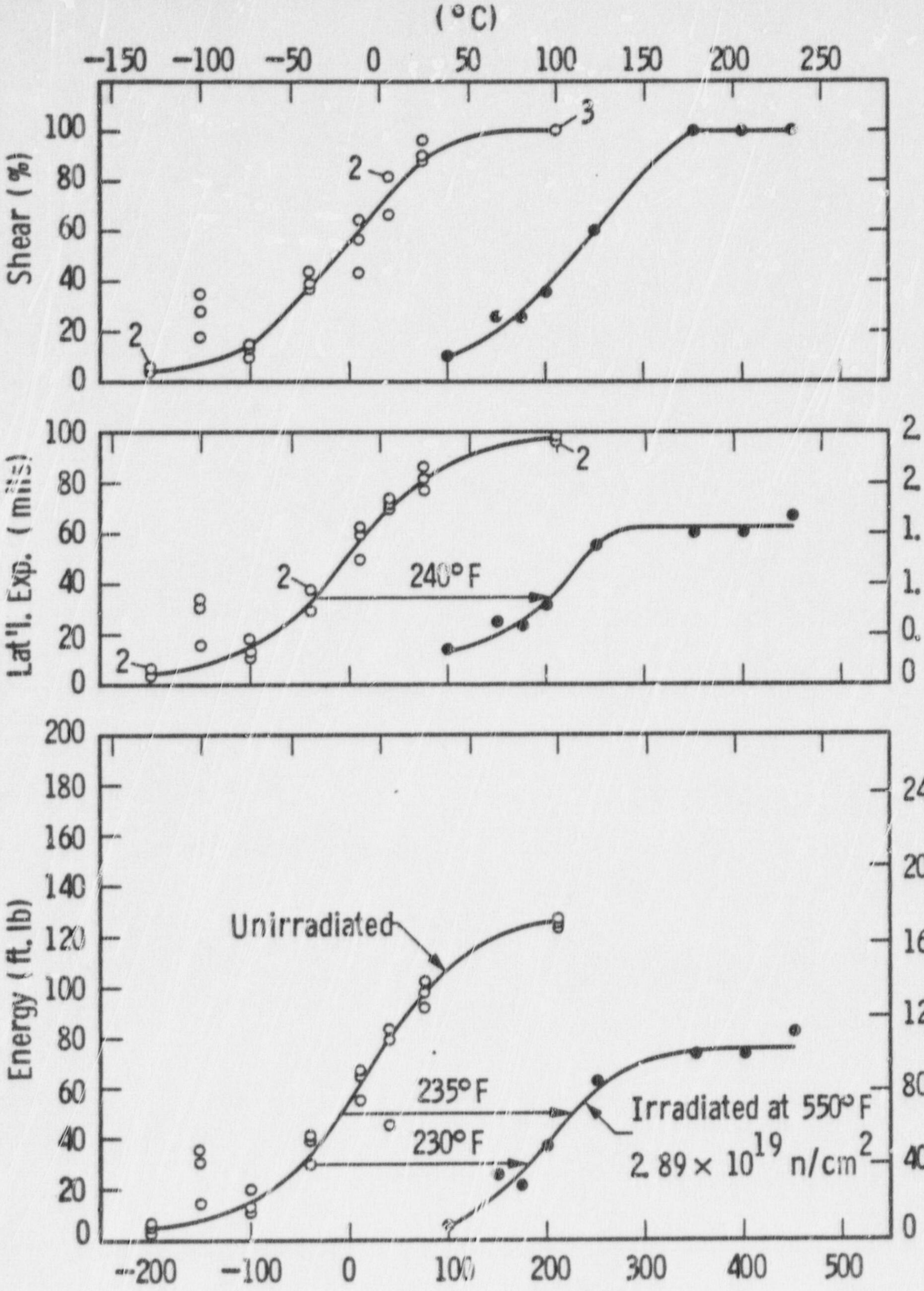

Figure 5-3 Charpy V-notch Impact Properties for Kewaunee Reactor Vessel Weld Metal

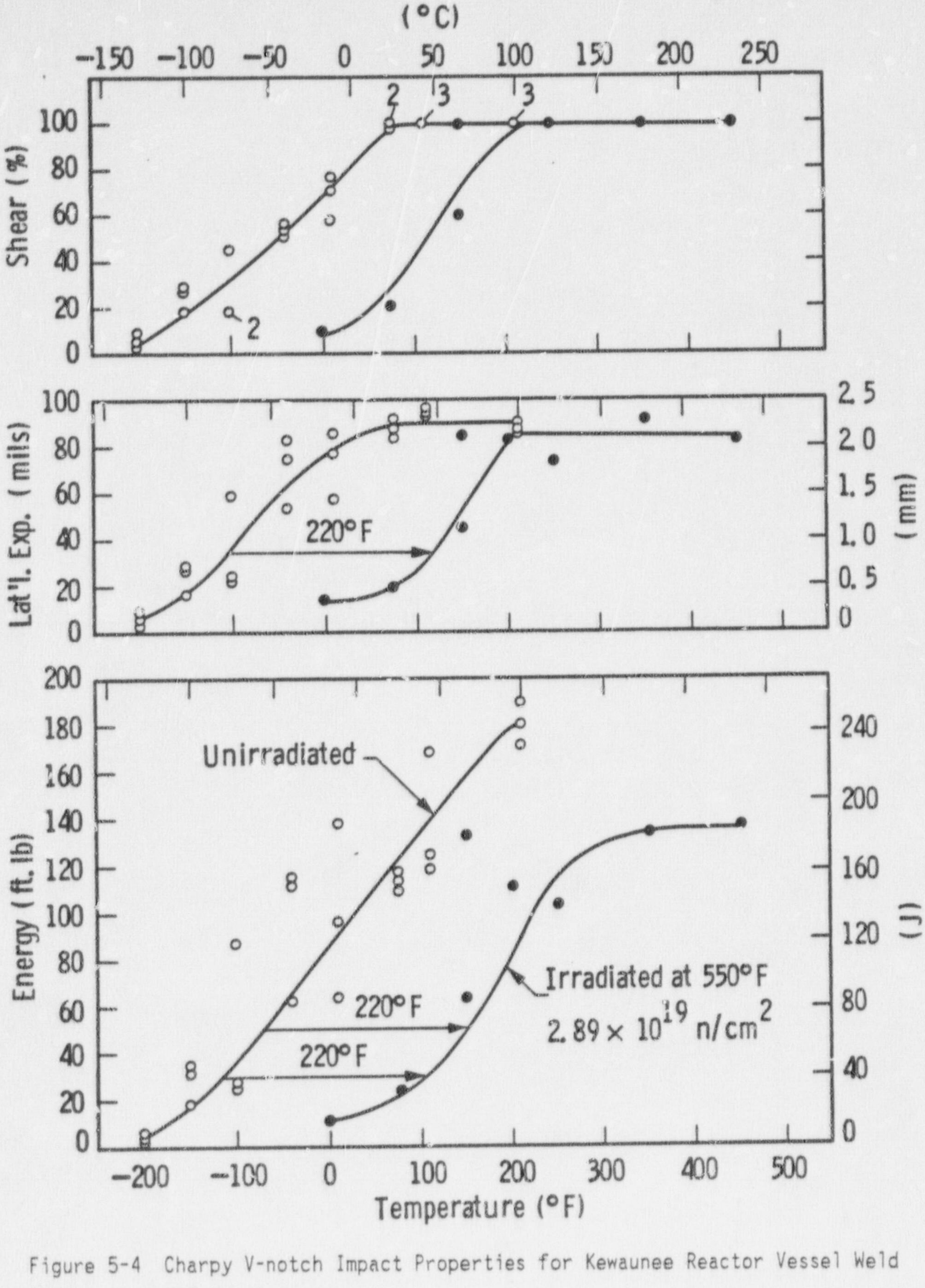

Figure 5-4 Charpy V-notch Impact Properties for Kewaunee Reactor Vessel Weld HAZ Metal

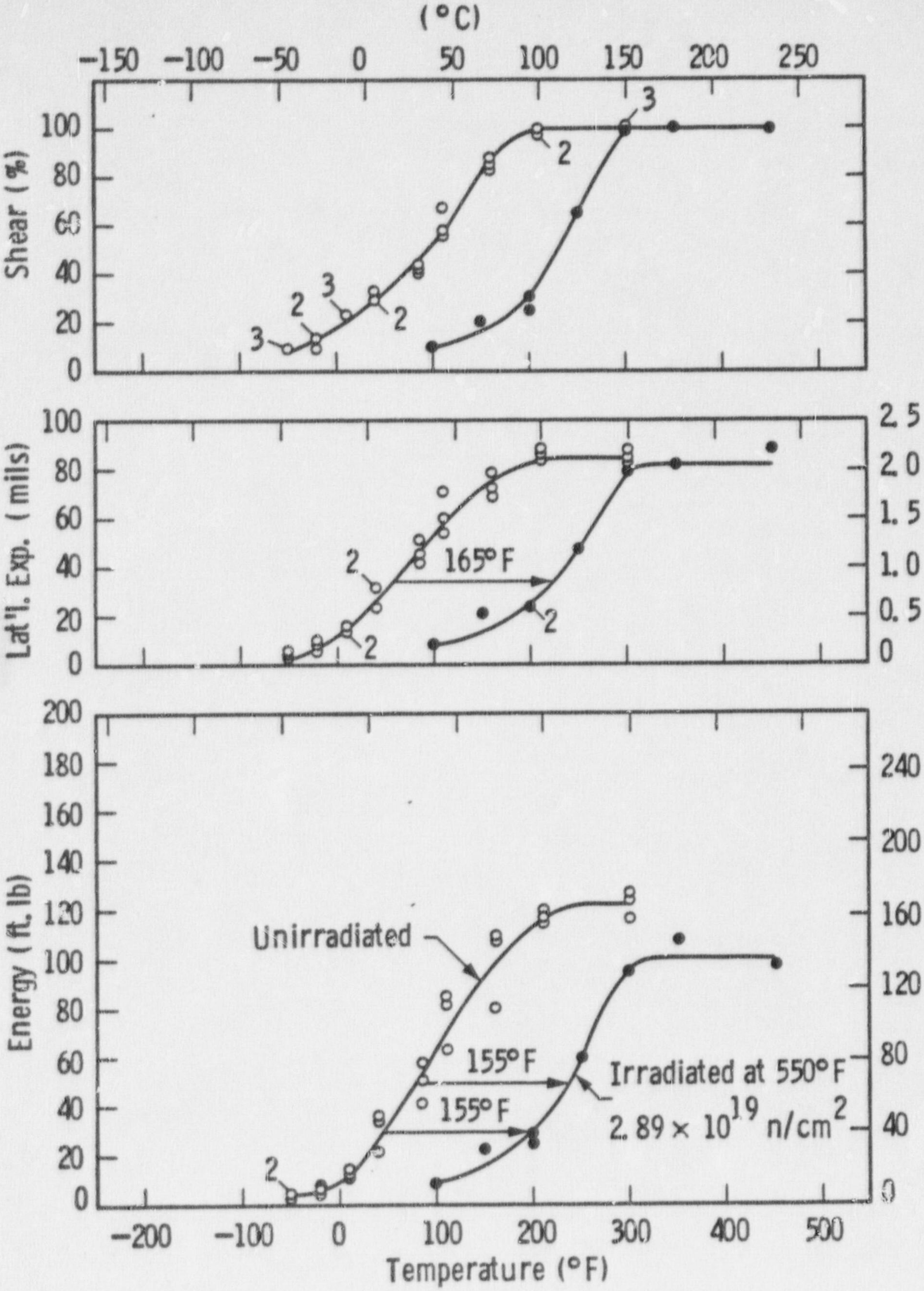

Figure 5-5 Charpy V-Notch Impact Properties for Kewaunee ASTM Correlation Monitor Material (HSST Plate 02)

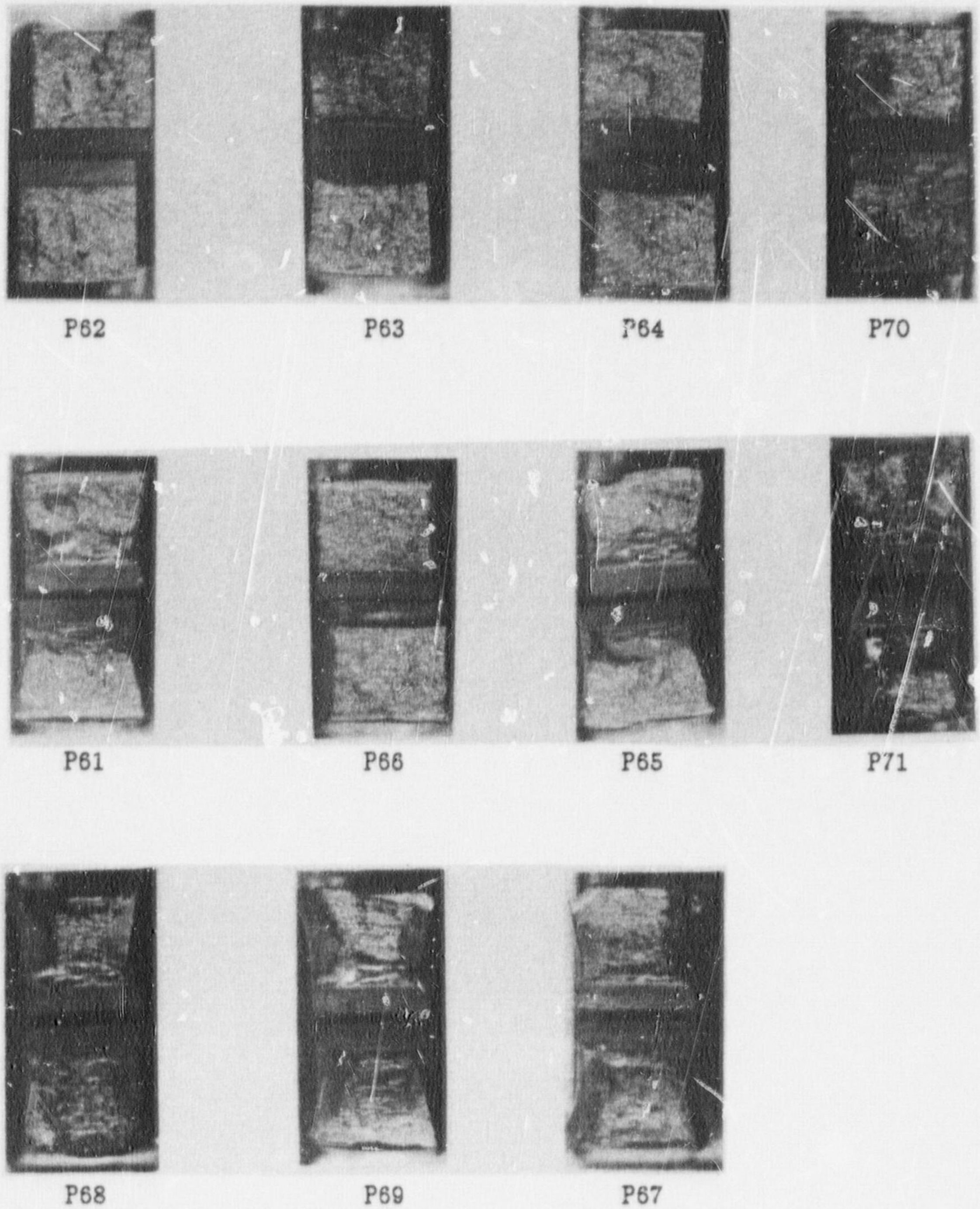

Figure 5-6 Charpy Impact Specimen Fracture Surfaces for Kewaunee Reactor Vessel Shell Forging 122X208 VA1 (Tangential Orientation)

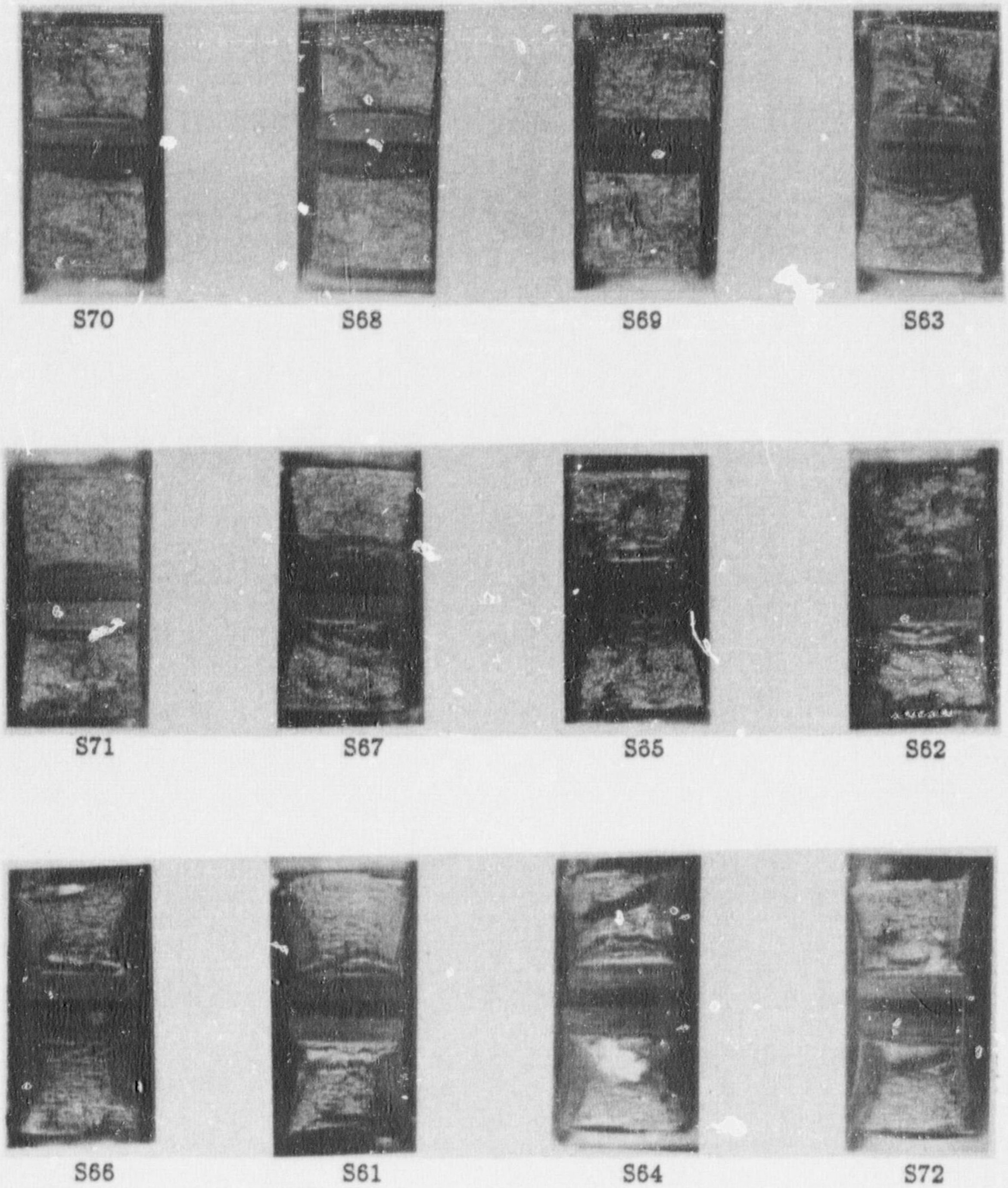

Figure 5-7 Charpy Impact Specimen Fracture Surfaces for Kewaunee Reactor Vessel Shell Forging 123X167 VA1 (Tangential Orientation)

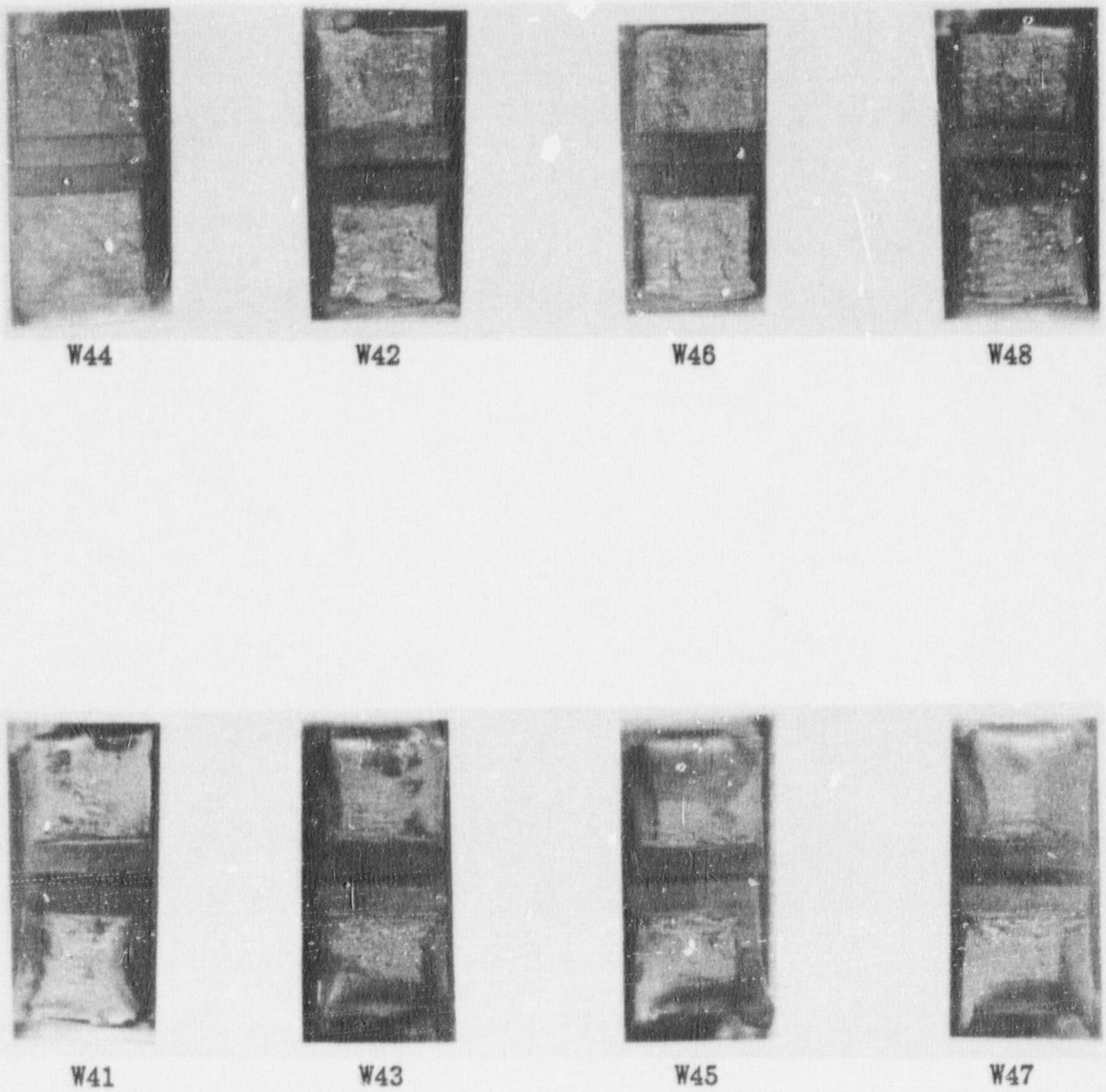

Figure 5-8 Charpy Impact Specimen Fracture Surfaces for Kewaunee Reactor Vessel Weld Metal

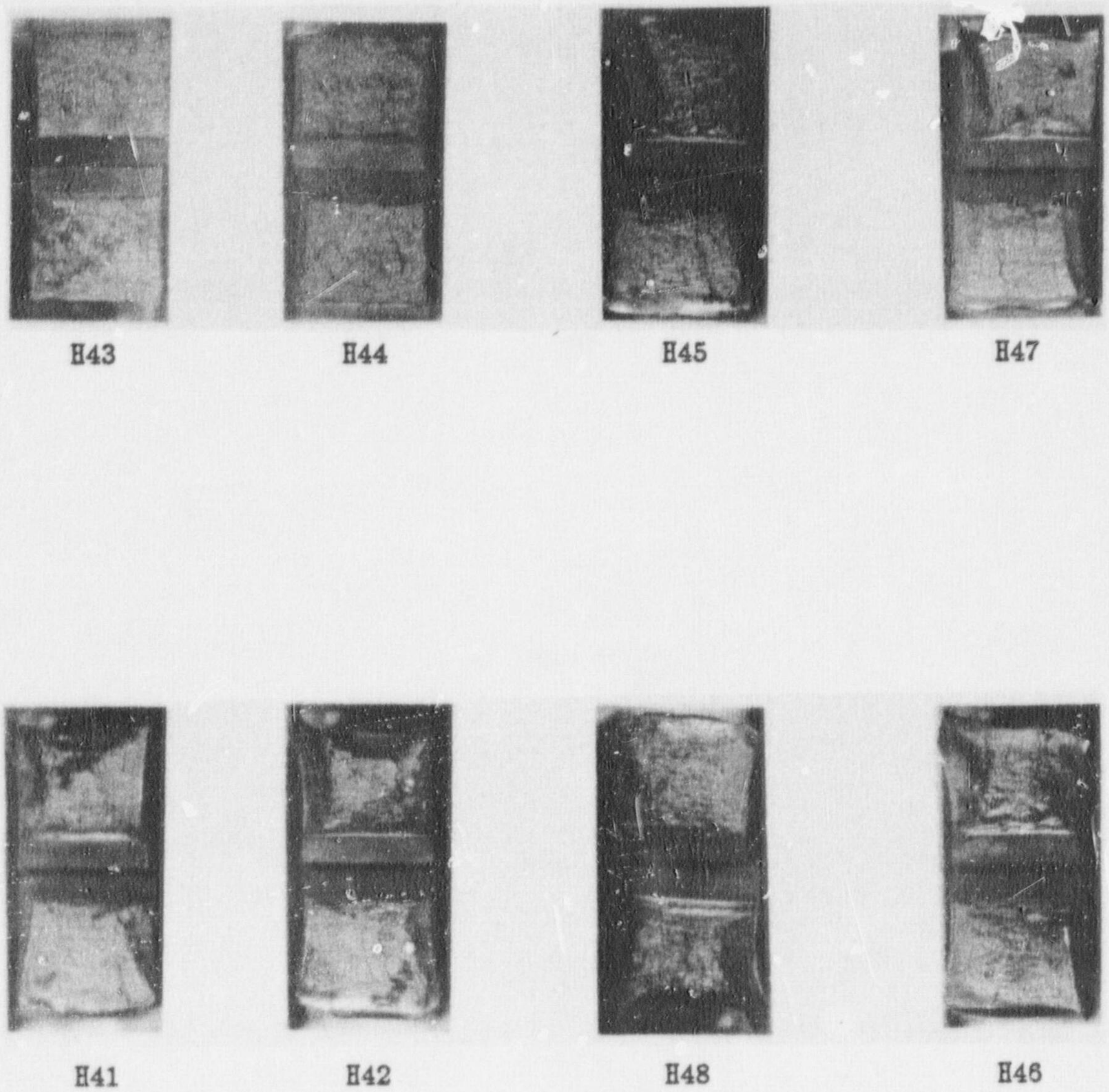

Figure 5-9 Charpy Impact Specimen Fracture Surfaces for Kewaunee Reactor Vessel HAZ Metal

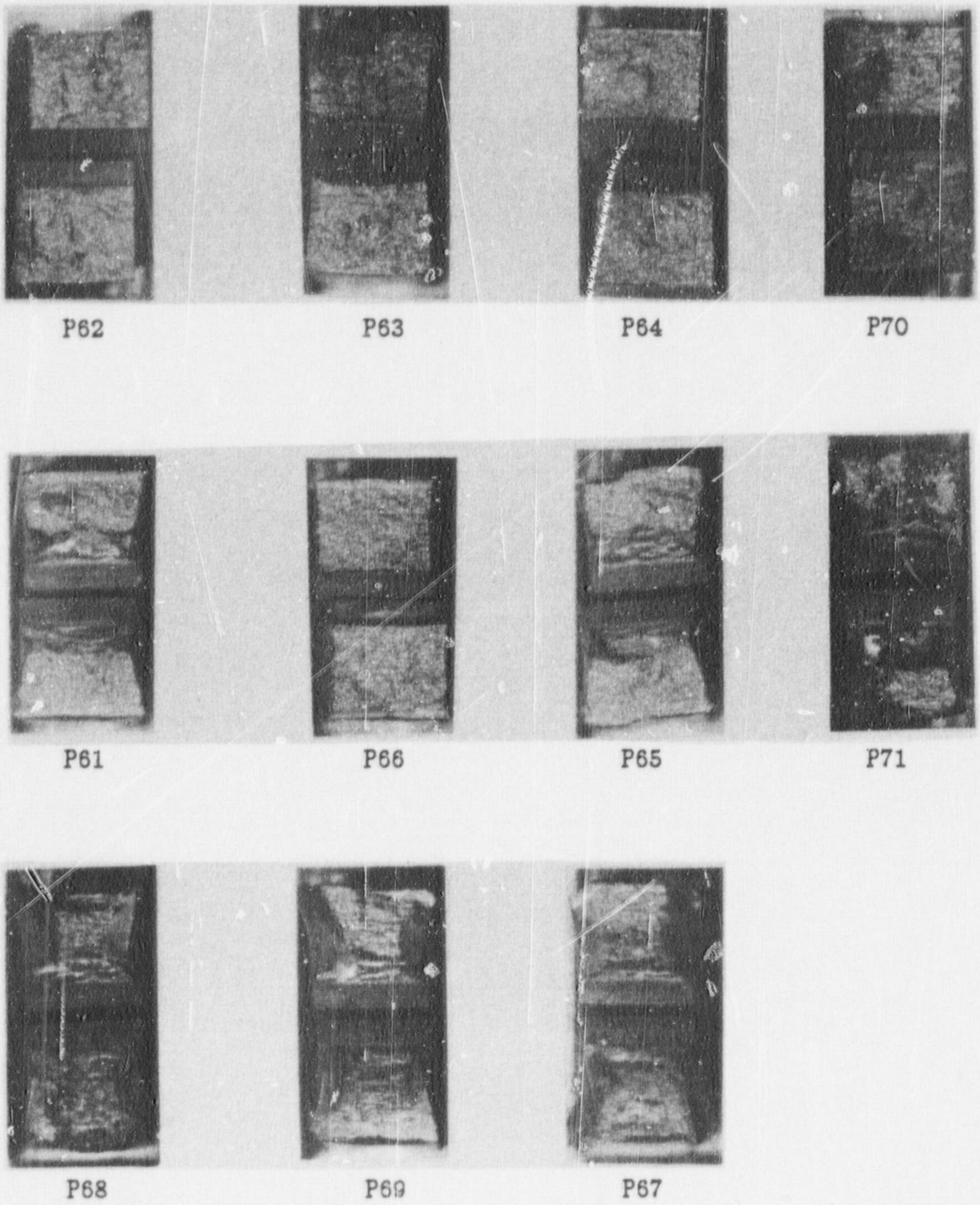

Figure 5-6 Charpy Impact Specimen Fracture Surfaces for Kewaunee Reactor Vessel Shell Forging 122X203 VA1 (Tangential Orientation)

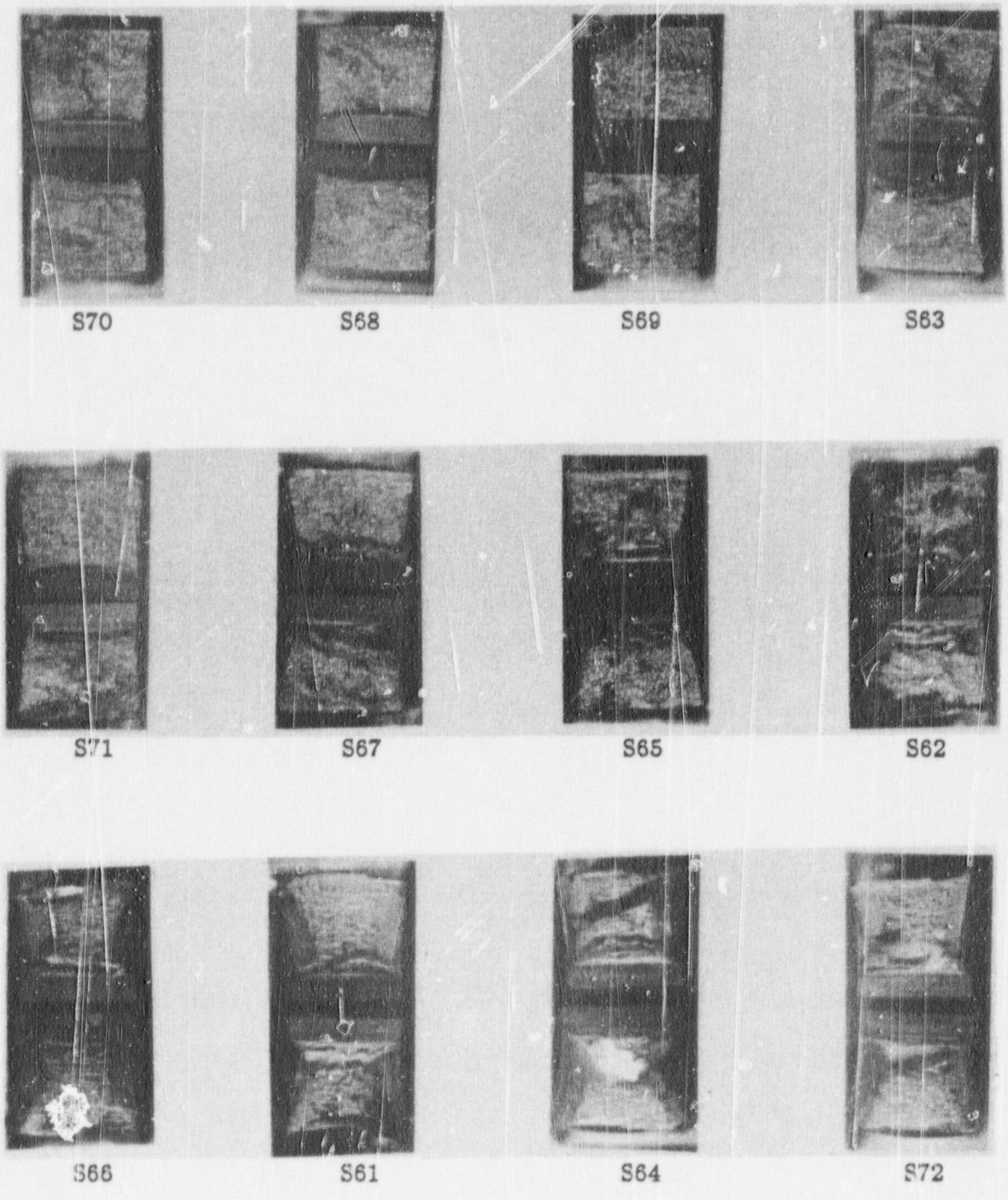

Figure 5-7 Charpy Impact Specimen Fracture Surfaces for Kewaunee Reactor Vessel Shell Forging 123X167 VA1 (Tangential Orientation)

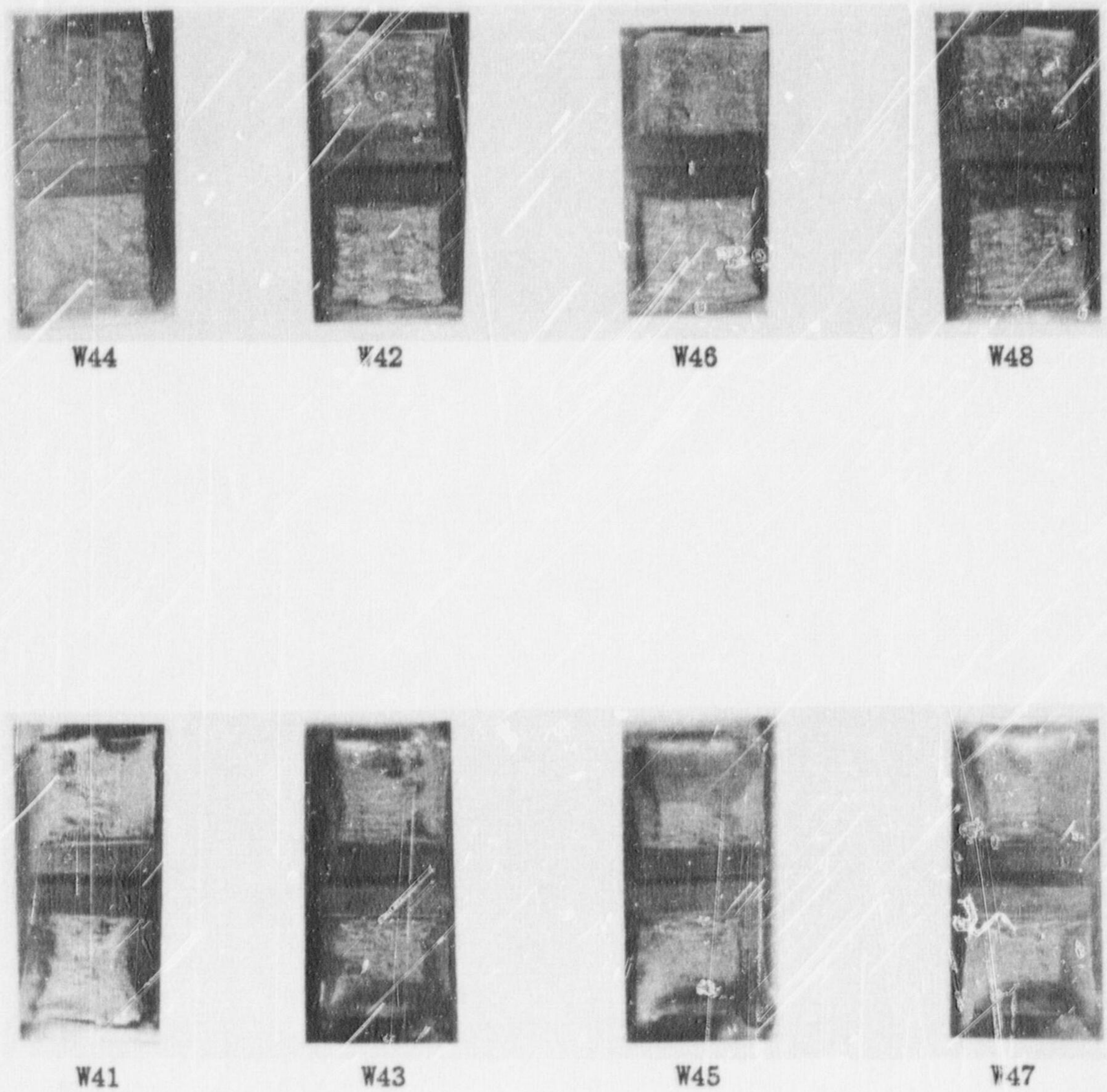

Figure 5-8 Charpy Impact Specimen Fracture Surfaces for Kewaunee Reactor Vessel Weld Metal

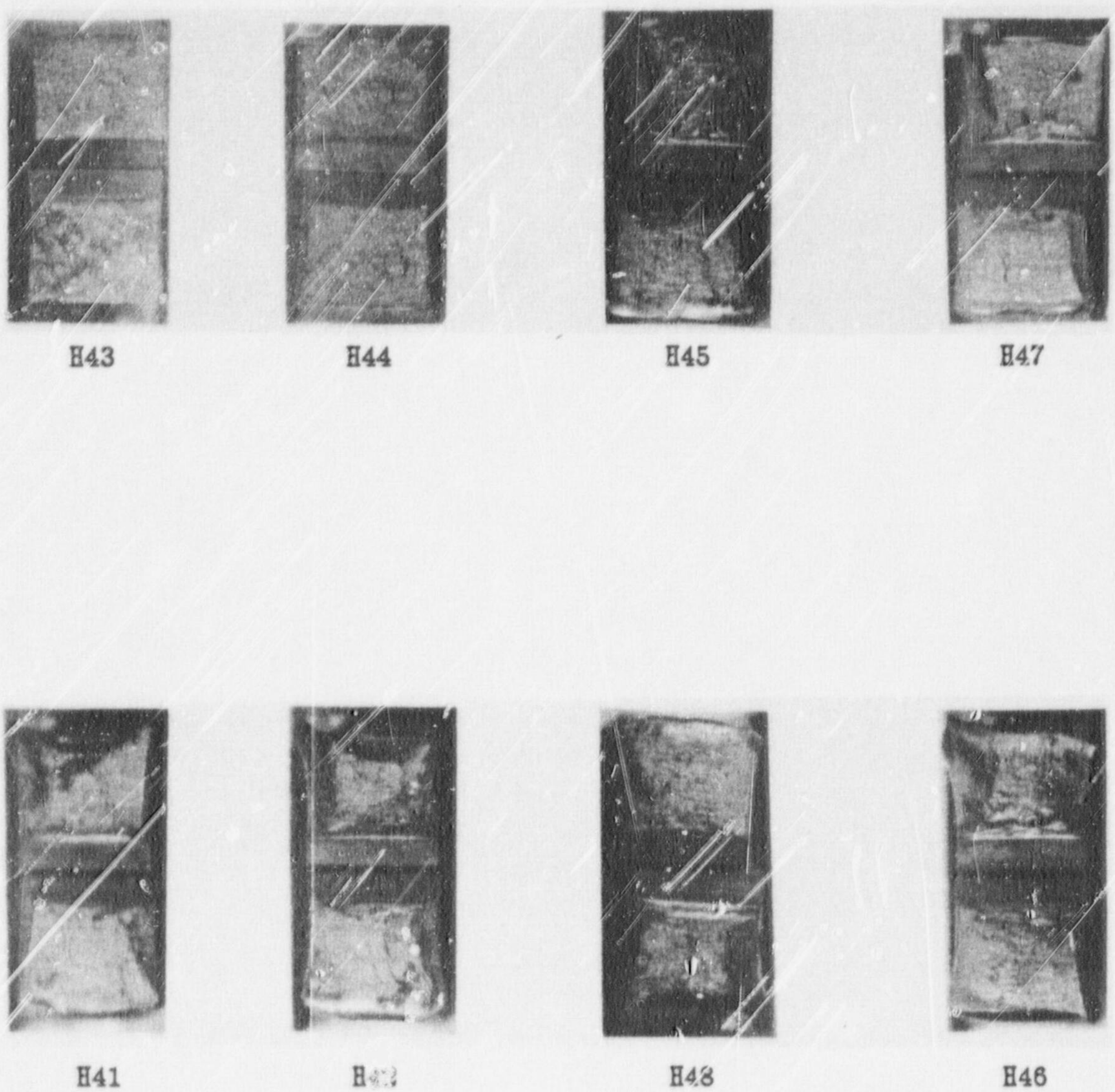

Figure 5-9 Charpy Impact Specimen Fracture Surfaces for Kewaunee Reactor Vessel HAZ Metal

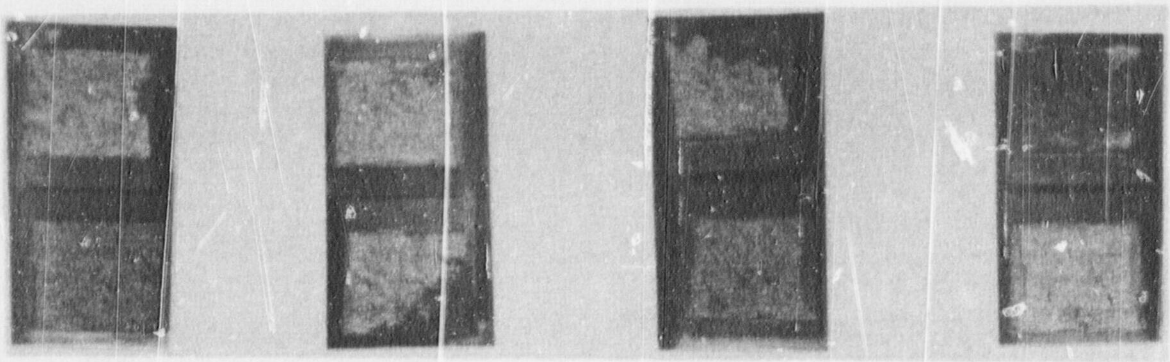

R41 R45 R46 R42

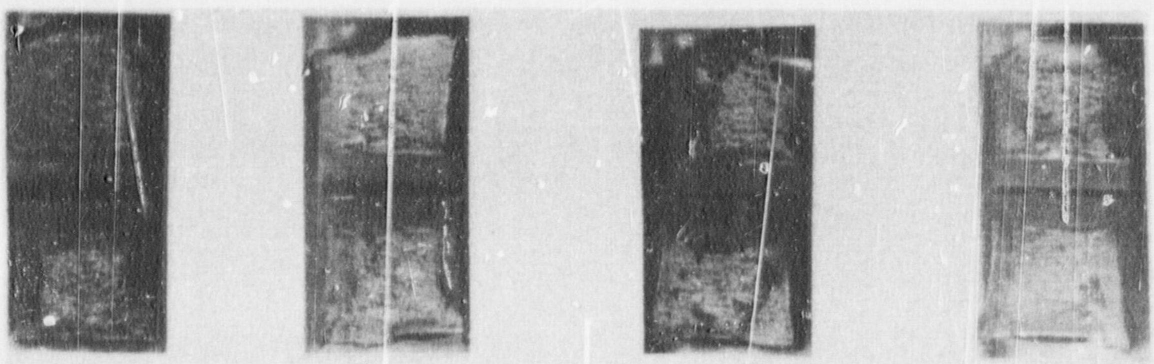

R47 R44 R48 R43

Figure 5-10 Charpy Impact Specimen Fracture Surfaces For Kewaunee ASTM Correlation Monitor Material (HSST Plate 02)

Curve 756428-A

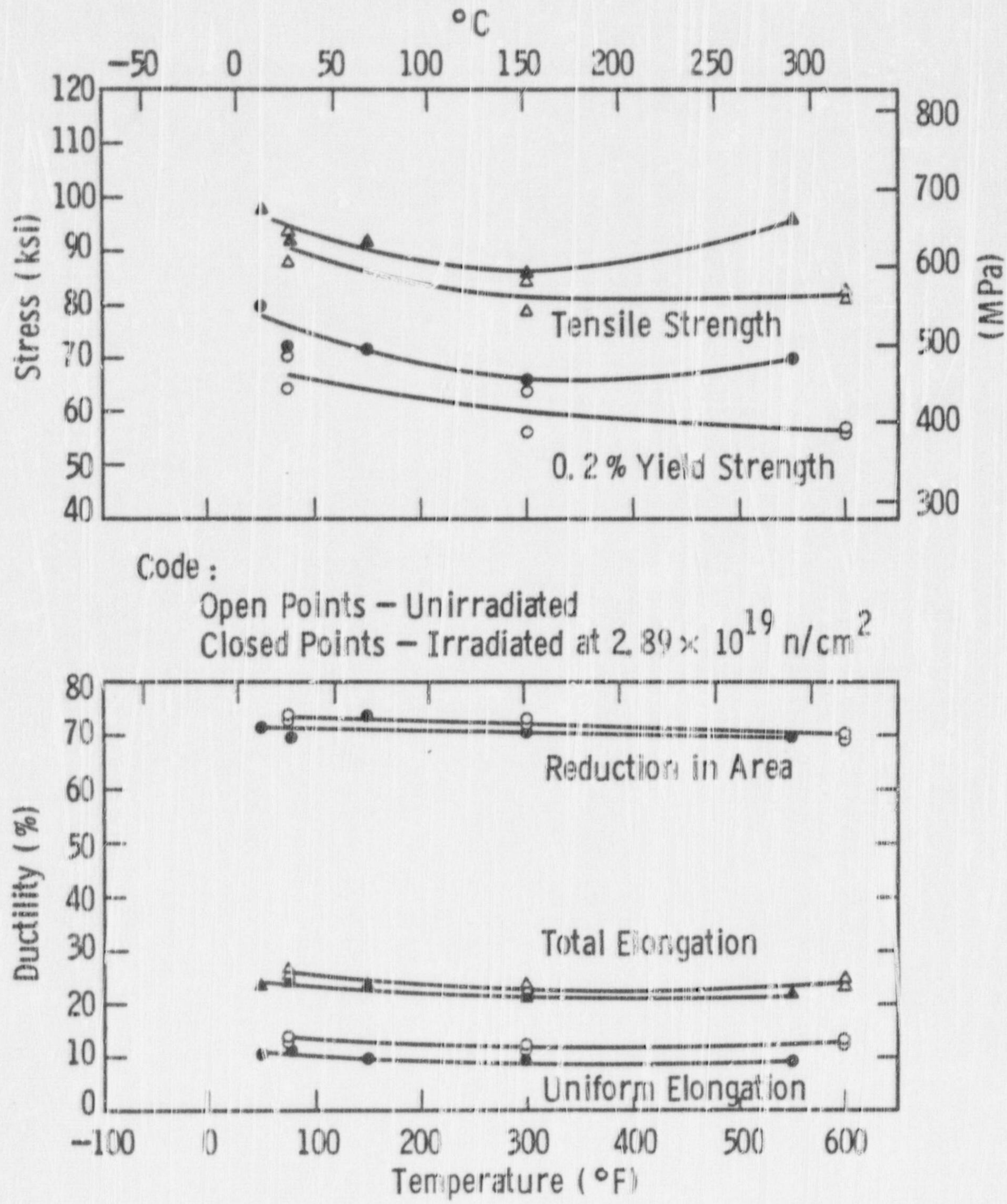

Figure 5-11 Tensile Properties for Kewaunee Reactor Vessel Shell Forging 122X208 VA1 (Tangential Orientation)

Curve 756437-A

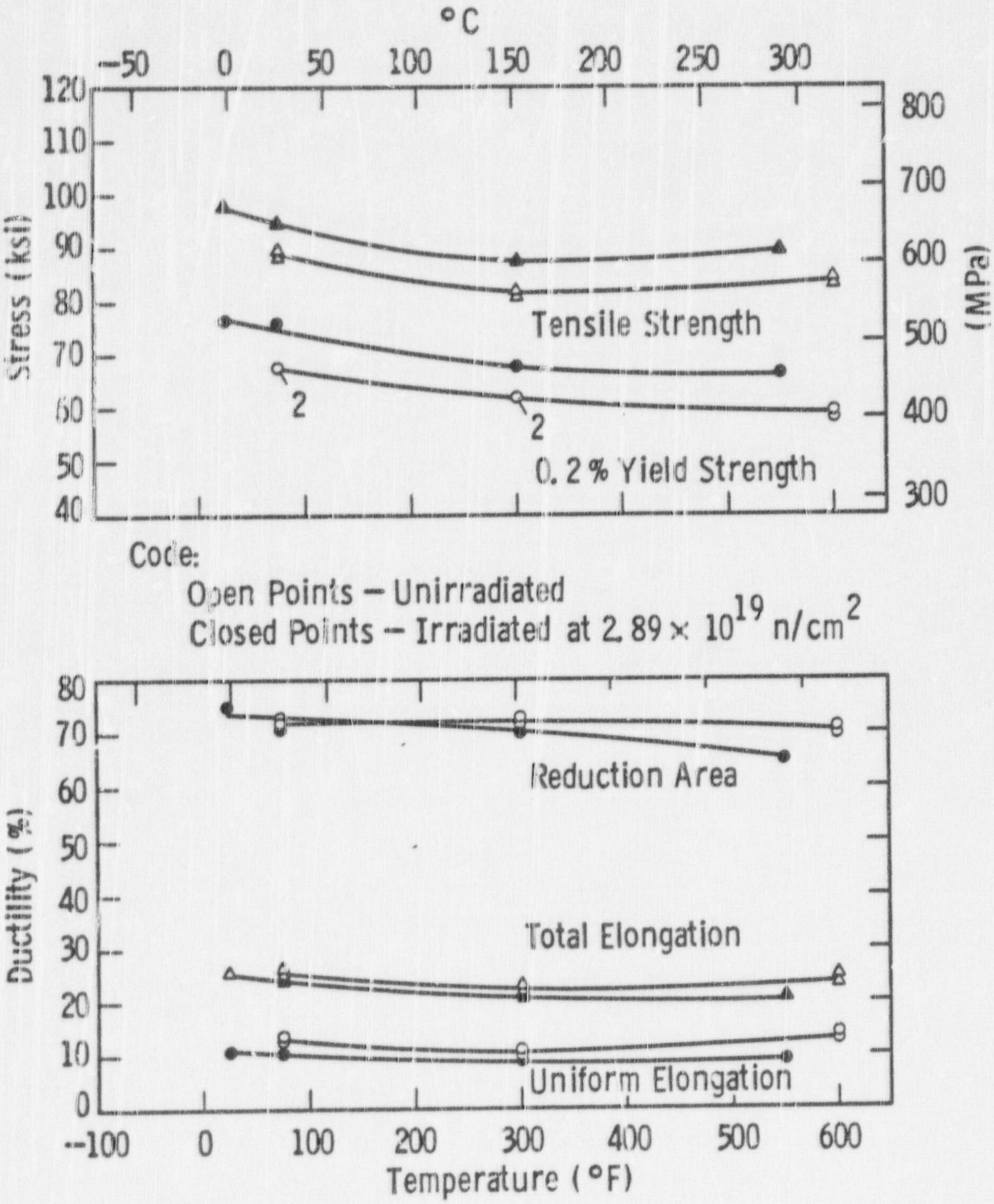

Figure 5-12 Tensile Properties for Kewaunee Reactor Vessel Shell Forging 123X167 VA1 (Tangential Orientation)

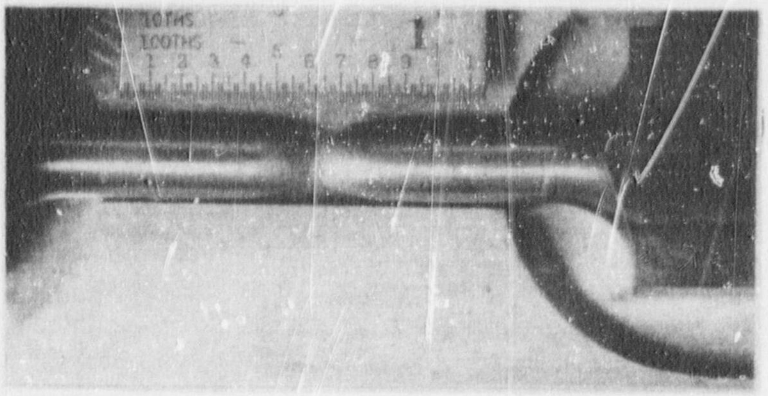

Specimen P27 **300°F**

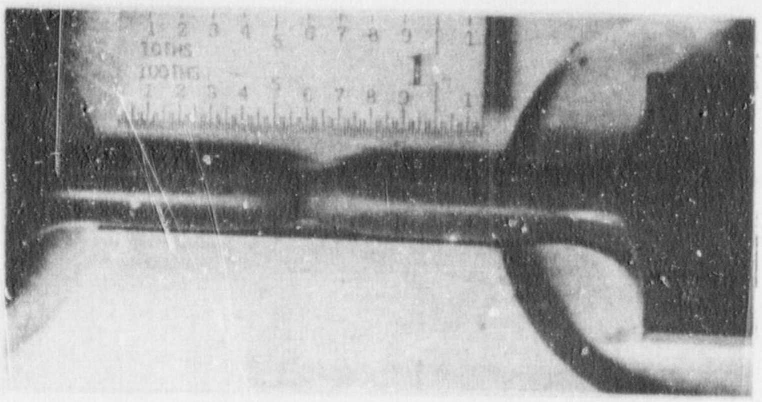

Specimen P24 **550°F**

Figure 5-13 (Continued)

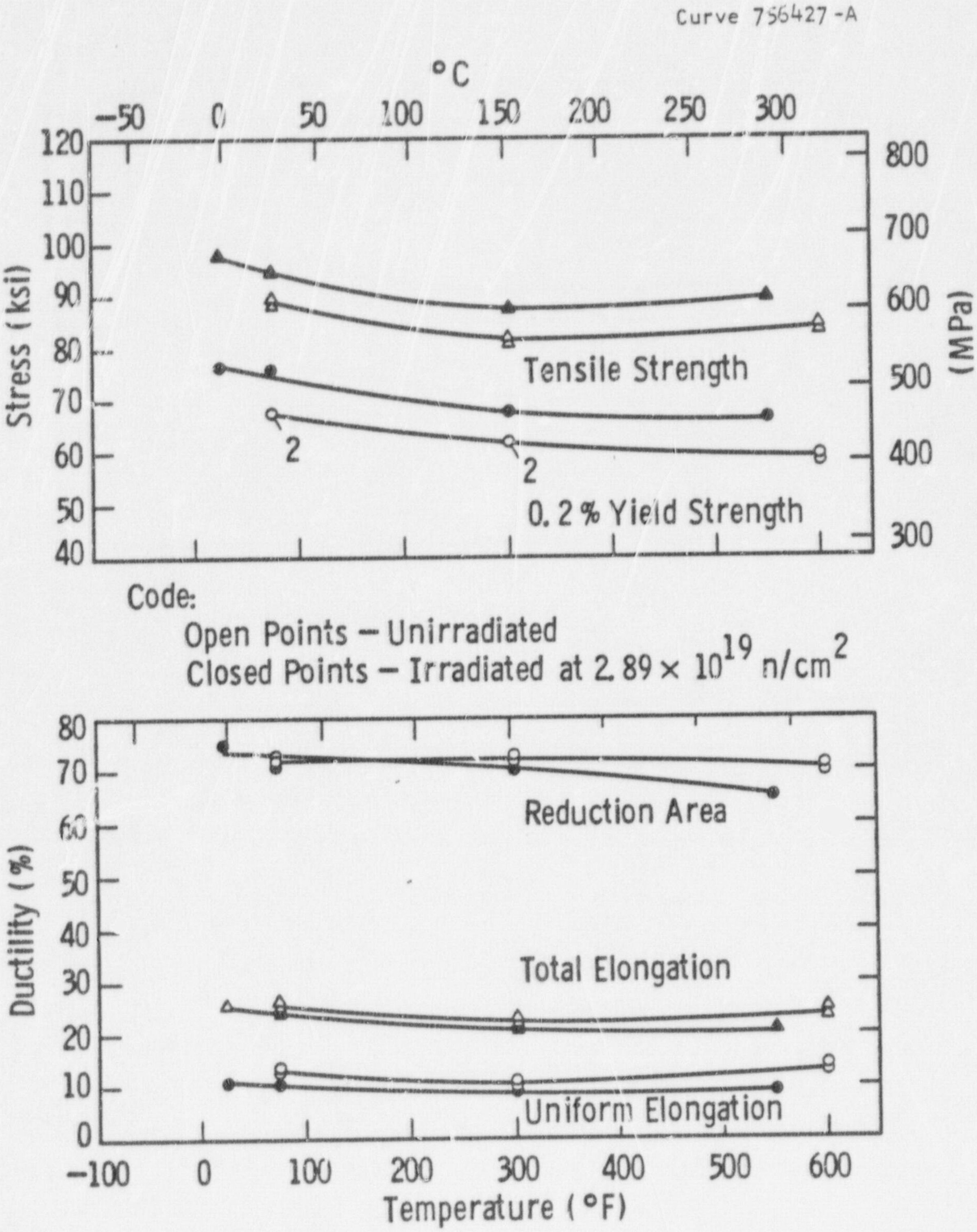

Figure 5-12 Tensile Properties for Kewaunee Reactor Vessel Shell Forging 123X167 VA1 (Tangential Orientation)

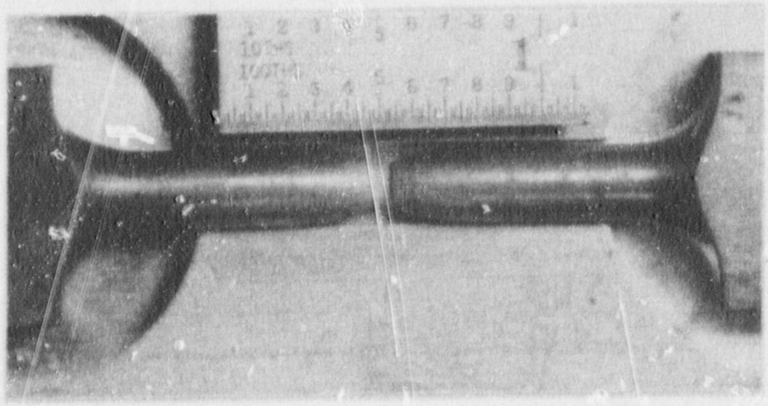

Specimen P25 50°F

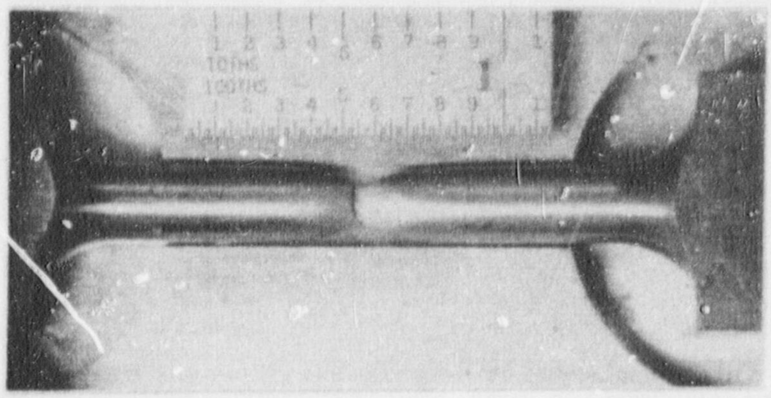

Specimen P26 78°F

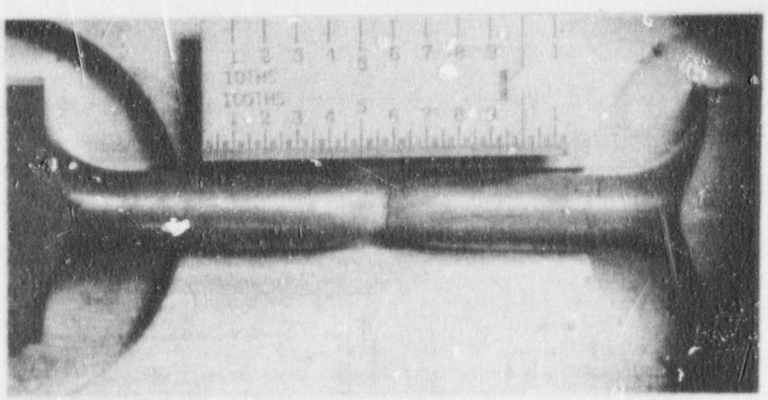

Specimen P23 150°F

Figure 5-13 Fractured Tensile Specimens from the Kewaunee Reactor Vessel Shell Forging 122X208 VA1 (Tangential Orientation)

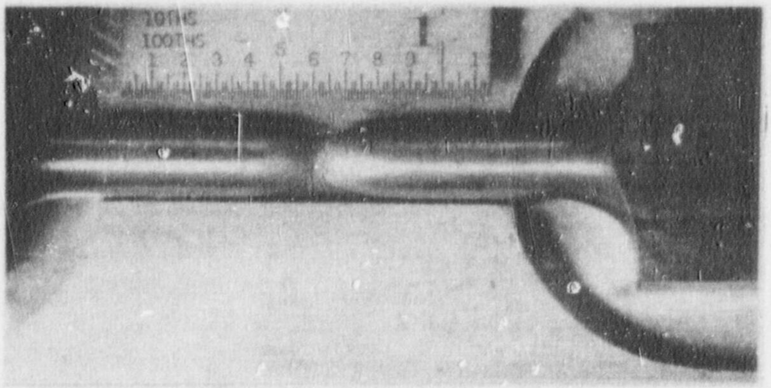

Specimen P27 300°F

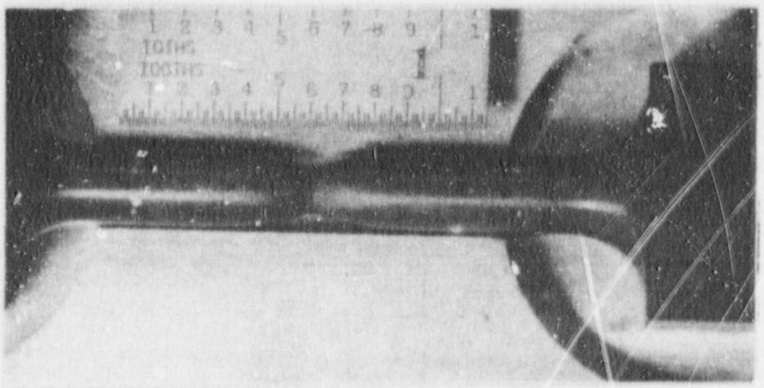

Specimen P24 550°F

Figure 5-13 (Continued)

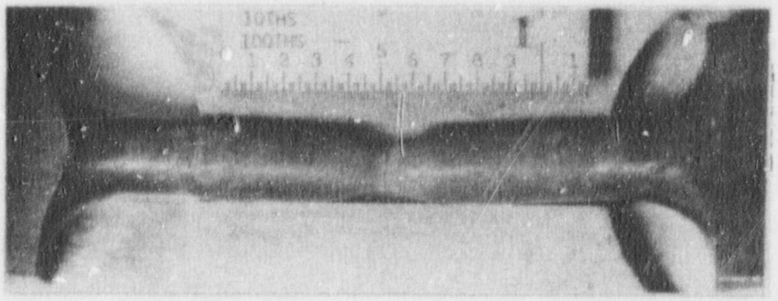

Specimen S21 **25°F**

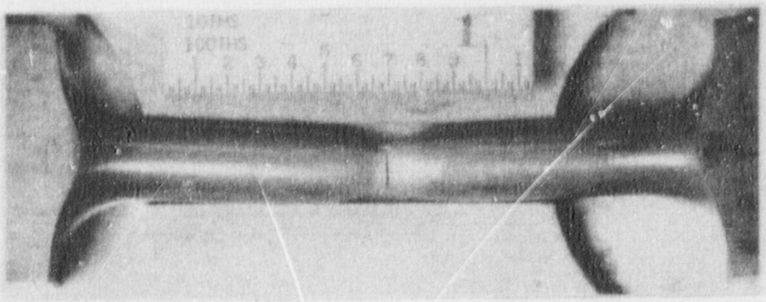

Specimen S19 **75°F**

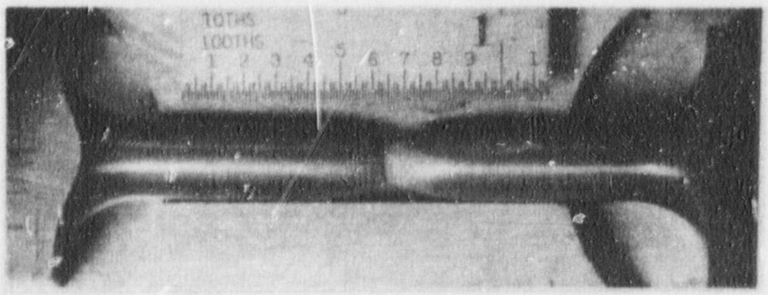

Specimen S20 **300°F**

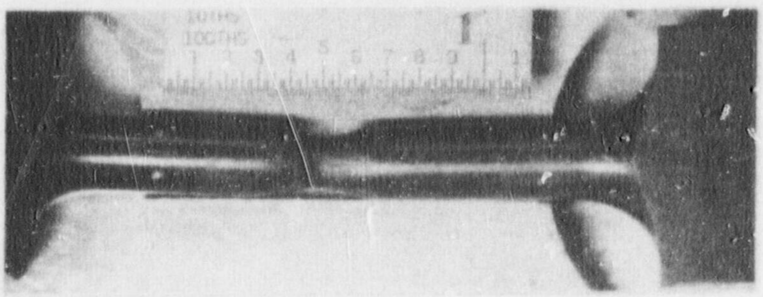

Specimen S18 **550°F**

Figure 5-14 Fractured Tensile Specimens from the Kewaunee Reactor Vessel Shell Forging 123X167 VA1 (Tangential Orientation)

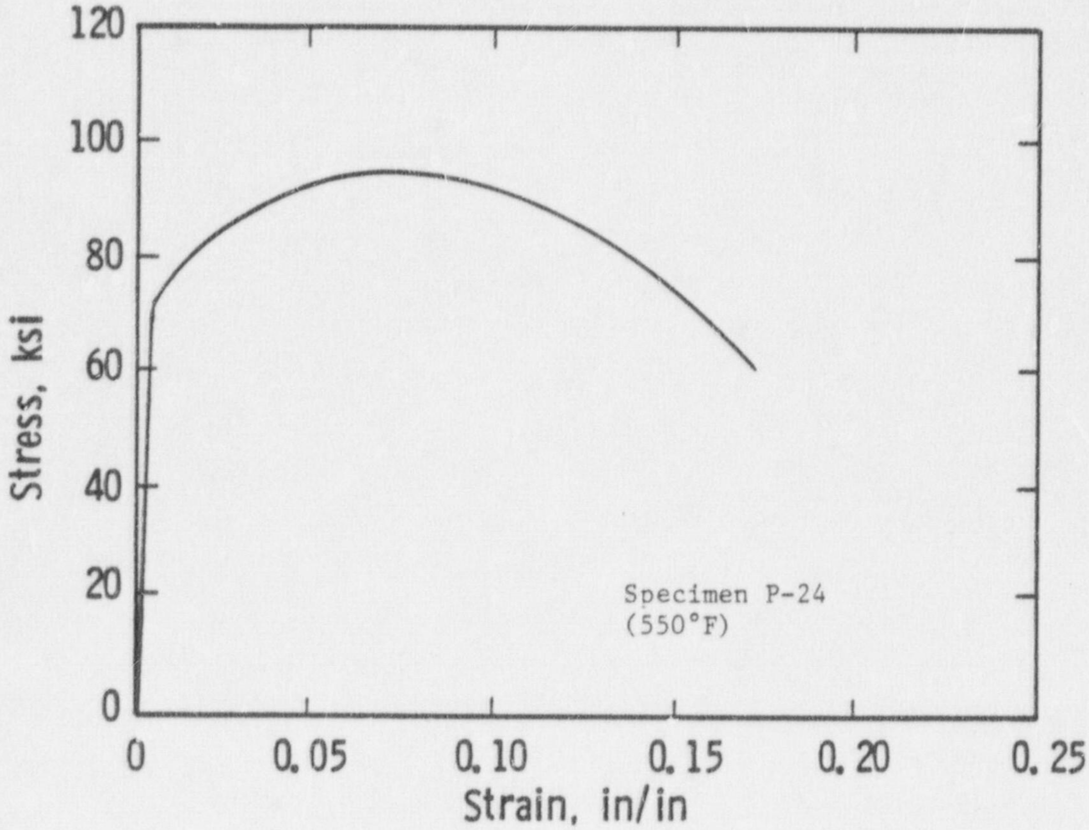

Figure 5-15. Typical Stress-Strain Curve for Tension Specimens

SECTION 6
RADIATION ANALYSIS AND NEUTRON DOSIMETRY

6.1 INTRODUCTION

Knowledge of the neutron environment within the reactor pressure vessel and surveillance capsule geometry is required as an integral part of LWR reactor pressure vessel surveillance programs for two reasons. First, in order to interpret the neutron radiation-induced material property changes observed in the test specimens, the neutron environment (energy spectrum, flux, fluence) to which the test specimens were exposed must be known. Second, in order to relate the changes observed in the test specimens to the present and future condition of the reactor vessel, a relationship must be established between the neutron environment at various positions within the reactor vessel and that experienced by the test specimens. The former requirement is normally met by employing a combination of rigorous analytical techniques and measurements obtained with passive neutron flux monitors contained in each of the surveillance capsules. The latter information is derived solely from analysis.

The use of fast neutron fluence ($E > 1.0$ MeV) to correlate measured materials properties changes to the neutron exposure of the material for light water reactor applications has traditionally been accepted for development of damage trend curves as well as for the implementation of trend curve data to assess vessel condition. In recent years, however, it has been suggested that an exposure model that accounts for differences in neutron energy spectra between surveillance capsule locations and positions within the vessel wall could lead to an improvement in the uncertainties associated with damage trend curves as well as to a more accurate evaluation of damage gradients through the pressure vessel wall.

Because of this potential shift away from a threshold fluence toward an energy dependent damage function for data correlation, ASTM Standard Practice E853, "Analysis and Interpretation of Light Water Reactor Surveillance Results," recommends reporting displacements per iron atom (dpa) along with fluence (E > 1.0 MeV) to provide a data base for future reference [6]. The energy dependent dpa function to be used for this evaluation is specified in ASTM Standard Practice E693, "Characterizing Neutron Exposures in Ferritic Steels in Terms of Displacements per Atom." The application of the dpa parameter to the assessment of embrittlement gradients through the thickness of the pressure vessel wall has already been promulgated in Revision 2 to the Regulatory Guide 1.99, "Radiation Embrittlement of Reactor Vessel Materials."

This section provides the results of the neutron dosimetry evaluations performed in conjunction with the analysis of test specimens contained in surveillance capsule P. Fast neutron exposure parameters in terms of fast neutron fluence (E > 1.0 MeV), fast neutron fluence (E > 0.1 Mev), and iron atom displacements (dpa) are established for the capsule irradiation history. The analytical formalism relating the measured capsule exposure to the exposure of the vessel wall is described and used to project the integrated exposure of the vessel itself. Also uncertainties associated with the derived exposure parameters at the surveillance capsule and with the projected exposure of the pressure vessel are provided.

6.2 DISCRETE ORDINATES ANALYSIS

A plan view of the reactor geometry at the core midplane is shown in Figure 4-1. Six irradiation capsules attached to the thermal shield are included in the reactor design to constitute the reactor vessel surveillance program. The capsules are located at azimuthal angles of 77°, 67°, 57°, 257°, 247°, and 237° relative to the core cardinal area as shown in figure 4-1.

A plan view of a surveillance capsule holder attached to the thermal shield is shown in figure 6-1. The stainless steel specimen containers are 1-inch square and approximately 64 inches in height. The containers are positioned axially such that the specimens are centered on the core midplane, thus spanning the central 5.33 feet of the 12-foot high reactor core.

From a neutron transport standpoint, the surveillance capsule structures are significant. They have a marked effect on both the distribution of neutron flux and the neutron energy spectrum in the water annulus between the thermal shield and the reactor vessel. In order to properly determine the neutron environment at the test specimen locations, the capsules themselves must be included in the analytical model.

In performing the fast neutron exposure evaluations for the surveillance capsules and reactor vessel, two distinct sets of transport calculations were carried out. The first, a single computation in the conventional forward mode, was used primarily to obtain relative neutron energy distributions throughout the reactor geometry as well as to establish relative radial distributions of exposure parameters {$\phi(E > 1.0$ Mev,) $\phi(E > 0.1$ Mev), and dpa} through the vessel wall. The neutron spectral information was required for the interpretation of neutron dosimetry withdrawn from the surveillance capsule as well as for the determination of exposure parameter ratios; i.e., dpa/$\phi(E > 1.0$ MeV), within the pressure vessel geometry. The relative radial gradient information was required to permit the projection of measured exposure parameters to locations interior to the pressure vessel wall; i.e., the 1/4T, 1/2T, and 3/4T locations.

The second set of calculations consisted of a series of adjoint analyses relating the fast neutron flux (E > 1.0 MeV) at surveillance capsule positions, and several azimuthal locations on the pressure vessel inner radius to neutron source distributions within the reactor core. The importance functions generated from these adjoint analyses provided the basis for all absolute exposure projections and comparison with measurement. These importance functions, when combined with plant specific neutron source distributions, yielded absolute predictions of neutron exposure at the locations of interest and established the means to perform similar predictions and dosimetry evaluations for future exposure.

The absolute plant specific data from the adjoint evaluations together with relative neutron energy spectra and radial distribution information from the forward calculation provided the means to:

1. Evaluate neutron dosimetry obtained from surveillance capsule locations.

2. Extrapolate dosimetry results to key locations at the inner radius and through the thickness of the pressure vessel wall.

3. Enable a direct comparison of analytical prediction with measurement.

The forward transport calculation for the reactor model summarized in figures 4-1 and 6-1 was carried out in R, θ geometry using the DOT two-dimensional discrete ordinates code [7] and the SAILOR cross-section library [8]. The SAILOR library is a 47 group ENDFB-IV based data set produced specifically for light water reactor applications. In these analyses anisotopic scattering was treated with a P_3 expansion of the cross-sections and the angular discretization was modeled with an S_8 order of angular quadrature.

The reference core power distribution utilized in the forward analysis was derived from statistical studies of long-term operation of Westinghouse 2-loop plants. Inherent in the development of this reference core power distribution is the use of an out-in fuel management strategy; i.e., fresh fuel on the core periphery. Furthermore, for the peripheral fuel assemblies, a 2σ uncertainty derived from the statistical evaluation of plant to plant and cycle to cycle variations in peripheral power was used. Since it is unlikely that a single reactor would have a power distribution at the nominal $+2\sigma$ level for a large number of fuel cycles, the use of this reference distribution is expected to yield somewhat conservative results.

All adjoint analyses were also carried out using an S_8 order of angular quadrature and the P_3 cross-section approximation from the SAILOR library. Adjoint source locations were chosen at several azimuthal locations along the pressure vessel inner radius as well as the geometric center of each surveillance capsule. Again, these calculations were run in R, Θ geometry to provide neutron source distribution importance functions for the exposure parameter of interest; in this case, ϕ (E > 1.0 MeV). Having the importance functions and appropriate core source distributions, the response of interest could be calculated as:

$$R(r, \Theta) = \int_r \int_\Theta \int_E I(r, \Theta, E)\, S(r, \Theta, E)\, r\, dr\, d\Theta\, dE$$

where: $R(r, \Theta)$ = ϕ (E > 1.0 MeV) at radius r and azimuthal angle Θ

$I(r, \Theta, E)$ = Adjoint importance function at radius, r, azimuthal angle Θ, and neutron source energy E.

$S(r, \Theta, E)$ = Neutron source strength at core location r, Θ and energy E.

Although the adjoint importance functions used in the analysis were based on a response function defined by the threshold neutron flux (E > 1.0 MeV), prior calculations have shown that, while the implementation of low leakage loading patterns significantly impact the magnitude and the spatial distribution of the neutron field, changes in the relative neutron energy spectrum are of second order. Thus, for a given location the ratio of dpa/ϕ (E > 1.0 MeV) is insensitive to changing core source distributions. In the application of these adjoint important functions to the Kewaunee reactor, therefore, calculation of the iron displacement rates (dpa) and the neutron flux (E > 0.1 MeV) were computed on a plant specific basis by using dpa/ϕ (E > 1.0 MeV) and ϕ (E > 0.1 MeV)/ϕ (E > 1.0 MeV) ratios from the forward analysis in conjunction with the plant specific ϕ (E > 1.0 MeV) solutions from the individual adjoint evaluations.

The reactor core power distribution used in the plant specific adjoint calculations represented a time weighted average over the first 13 fuel cycles.

Selected results from the neutron transport analyses performed for the Kewaunee reactor are provided in tables 6-1 through 6-5. The data listed in these tables establish the means for absolute comparisons of analysis and measurement for the capsule irradiation period and provide the means to correlate dosimetry results with the corresponding neutron exposure of the pressure vessel wall.

In table 6-1, the calculated exposure parameters (ϕ (E > 1.0 MeV), ϕ (E > 0.1 MeV), and dpa) are given at the geometric center of surveillance capsule P using plant specific core power distributions and averaging over cycles 1-13. These plant specific data, based on the adjoint transport analysis, are meant to establish the absolute comparison of measurement with analysis and to provide an evaluation of the more recent loading patterns appropriate for projecting into the future. Similar data are given in table 6-2 for the pressure vessel inner radius. Again, the three pertinent exposure parameters are listed for the cycle 1-13 average plant specific power distributions. It is important to note that the data for the vessel inner radius were taken at the clad/base metal interface; and, thus, represent the maximum exposure levels of the vessel wall itself.

Radial gradient information for neutron flux (E > 1.0 MeV), neutron flux (E > 0.1 MeV), and iron atom displacement rate is given in tables 6-3, 6-4, and 6-5, respectively. The data, obtained from the forward neutron transport calculation, are presented on a relative basis for each exposure parameter at several azimuthal locations. Exposure parameter distributions within the wall may be obtained by normalizing the calculated or projected exposure at the vessel inner radius to the gradient data given in tables 6-3 through 6-5.

For example, the neutron flux (E > 1.0 MeV) at the 1/4T position on the 0° azimuth is given by:

$$\phi_{1/4T}(0°) = \phi(168.04, 0°) \; F \; (172.23, 0°)$$

where $\phi_{1/4T}(0°)$ = Projected neutron flux at the 1/4T position on the 0° azimuth

ϕ (168.04, 0°) = Projected or calculated neutron flux at the vessel inner radius on the 0° azimuth.

F (172.23, 0°) = Relative radial distribution function from table 6-3.

Similar expressions apply for exposure parameters in terms of $\phi(E > 0.1 \text{ MeV})$ and dpa/sec.

6.3 NEUTRON DOSIMETRY

The passive neutron sensors included in the Kewaunee surveillance program are listed in table 6-6. Also given in table 6-6 are the primary nuclear reactions and associated nuclear constants that were used in the evaluation of the neutron energy spectrum within the capsule and the subsequent determination of the various exposure parameters of interest {ϕ (E > 1.0 Mev), ϕ (E > 0.1 MeV), dpa}.

The relative locations of the neutron sensors within the capsules are shown in figure 4-2. The iron, nickel, copper, and cobalt-aluminum monitors, in wire form, were placed in holes drilled in spacers at several axial levels within the capsules. The cadmium shielded neptunium and uranium fission monitors were accommodated within the dosimeter block located near the center of the capsule.

The use of passive monitors such as those listed in table 6-6 does not yield a direct measure of the energy dependent flux level at the point of interest. Rather, the activation or fission process is a measure of the integrated effect that the time- and energy-dependent neutron flux has on the target material over the course of the irradiation period. An accurate assessment of the average neutron flux level incident on the various monitors may be derived from the activation measurements only if the irradiation parameters are well known. In particular, the following variables are of interest:

- The specific activity of each monitor.
- The operating history of the reactor.
- The energy response of the monitor.
- The neutron energy spectrum at the monitor location.
- The physical characteristics of the monitor.

The specific activity of each of the neutron monitors was determined using established ASTM procedures [6, 9-21]. Following sample preparation and weighing, the activity of each monitor was determined by means of a lithium-drifted germanium, Ge(Li), gamma spectrometer. The irradiation history of the Kewaunee reactor during cycles 1-13 was obtained from NUREG-0020, "Licensed Operating Reactors Status Summary Report" for the applicable period.

The irradiation history applicable to capsule P is given in table 6-7. Measured and saturated reaction product specific activities as well as measured full power reaction rates are listed in table 6-8. Reaction rate values were derived using the pertinent data from tables 6-6 and 6-7.

Values of key fast neutron exposure parameters were derived from the measured reaction rates using the FERRET least squares adjustment code [22]. The FERRET approach used the measured reaction rate data and the calculated neutron energy spectrum at the center of the surveillance capsule as input and proceeded to adjust the a priori (calculated) group fluxes to produce a best fit (in a least squares sense) to the reaction rate data. The exposure parameters along with associated uncertainties were then obtained from the adjusted spectra.

In the FERRET evaluations, a log normal least-squares algorithm weights both the a priori values and the measured data in accordance with the assigned uncertainties and correlations. In general, the measured values f are linearly related to the flux ϕ by some response matrix A:

$$f_i^{(s,\alpha)} = \sum_g A_{ig}^{(s)} \phi_g^{(\alpha)}$$

where i indexes the measured values belonging to a single data set s, g designates the energy group and α delineates spectra that may be simultaneously adjusted. For example,

$$R_i = \sum_g \sigma_{ig} \phi_g$$

relates a set of measured reaction rates R_i to a single spectrum ϕ_g by the multigroup cross section σ_{ig}. (In this case, FERRET also adjusts the cross-sections.) The log normal approach automatically accounts for the physical constraint of positive fluxes, even with the large assigned uncertainties.

In the FERRET analysis of the dosimetry data, the continuous quantities (i.e., fluxes and cross-sections) were approximated in 53 groups. The calculated fluxes from the discrete ordinates analysis were expanded into the FERRET group structure using the SAND-II code [23]. This procedure was carried out by first expanding the a priori spectrum into the SAND-II 620 group structure using a SPLINE interpolation procedure for interpolation in regions where group boundaries do not coincide. The 620-point spectrum was then easily collapsed to the group scheme used in FERRET.

The cross-sections were also collapsed into the 53 energy-group structure using SAND II with calculated spectra (as expanded to 620 groups) as weighting functions. The cross sections were taken from the ENDF/B-V dosimetry file. Uncertainty estimates and 53 x 53 covariance matrices were constructed for each cross section. Correlations between cross sections were neglected due to data and code limitations, but are expected to be unimportant.

For each set of data or a priori values, the inverse of the corresponding relative covariance matrix M is used as a statistical weight. In some cases, as for the cross sections, a multigroup covariance matrix is used. More often, a simple parameterized form is used:

$$M_{gg'} = R_N^2 + R_g R_{g'} P_{gg'}$$

where R_N specifies an overall fractional normalization uncertainty (i.e., complete correlation) for the corresponding set of values. The fractional uncertainties R_g specify additional random uncertainties for group g that are correlated with a correlation matrix:

$$P_{gg'} = (1 - \theta)\, \delta_{gg'} + \theta \exp \left[\frac{-(g-g')^2}{2\gamma^2}\right]$$

The first term specifies purely random uncertainties while the second term describes short-range correlations over a range γ (θ specifies the strength of the latter term.)

For the a priori calculated fluxes, a short-range correlation of $\gamma = 6$ groups was used. This choice implies that neighboring groups are strongly correlated when θ is close to 1. Strong long-range correlations (or anticorrelations) were justified based on information presented by R. E. Maerker [24]. Maerker's results are closely duplicated when $\gamma = 6$. For the integral reaction rate covariances, simple normalization and random uncertainties were combined as deduced from experimental uncertainties.

Results of the FERRET evaluation of the capsule P dosimetry are given in table 6-9 The data summarized in table 6-9 indicated that the capsule received an integrated exposure of 2.89×10^{19} n/cm^2 (E > 1.0 MeV) with an associated uncertainty of $\pm$ 8%. Also reported are capsule exposures in terms of fluence (E > 0.1 MeV) and iron atom displacements (dpa). Summaries of the fit of the adjusted spectrum are provided in table 6-10. In general, excellent results were achieved in the fits of the adjusted spectrum to the individual experimental reaction rates. The adjusted spectrum itself is tabulated in table 6-11 for the FERRET 53 energy group structure.

A summary of the measured and calculated neutron exposure of capsule P is presented in table 6-12. The agreement between calculation and measurement falls within 7% for all fast neutron exposure parameters, whereas, the thermal neutron exposure calculated for capsule P was within 10% of the measured value.

Neutron exposure projections at key locations on the pressure vessel inner radius are given in table 6-13. Along with the current (11.08 EFPY) exposure derived from the capsule P measurements, projections are also provided for an exposure period to end of vessel design life (32 EFPY). The calculated exposure rates given in table 6-2 were used to perform projections beyond the end of cycle 13.

In the calculation of exposure gradients for use in the development of heatup and cooldown curves for the Kewaunee reactor coolant system, exposure projections to 20 EFPY and 32 EFPY were employed. Data based on both a fluence (E > 1.0 MeV) slope and a plant specific dpa slope through the vessel wall are provided in table 6-14. In order to access RT_{NDT} vs. fluence trend curves, dpa equivalent fast neutron fluence levels for the 1/4T and 3/4T positions were defined by the relations

$$\Phi' \ 1/4T = \Phi \ (\text{Surface}) \left\{ \frac{\text{dpa}(1/4T)}{\text{dpa (Surface)}} \right\}$$

$$\Phi' \ 3/4T = \Phi \ (\text{Surface}) \left\{ \frac{\text{dpa (3/4T)}}{\text{dpa (Surface)}} \right\}$$

Using this approach results in the dpa equivalent fluence values listed in table 6-14.

In table 6-15 updated lead factors are listed for each of the Kewaunee surveillance capsules. These data may be used as a guide in establishing future withdrawal schedules for the remaining capsules.

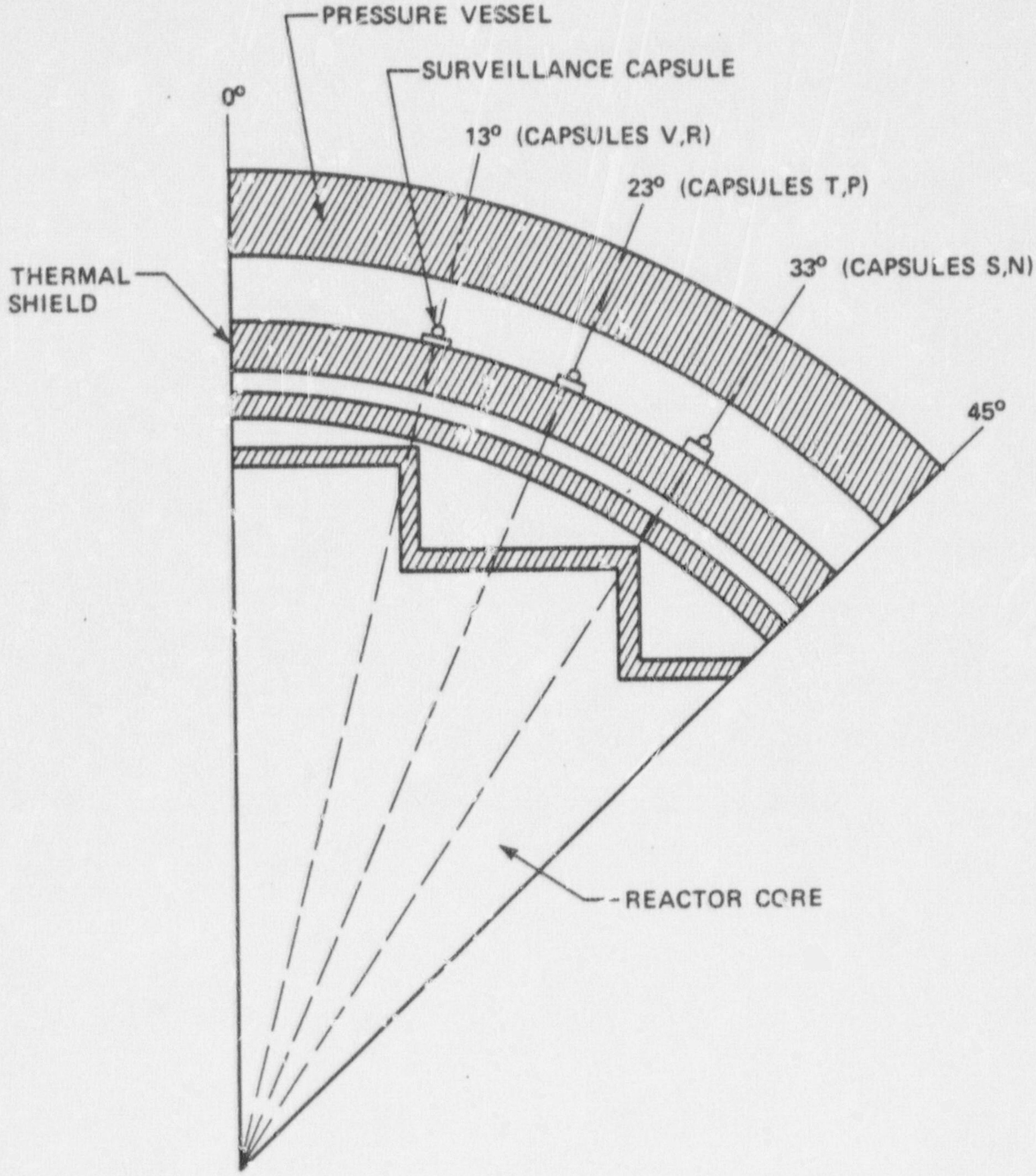

Figure 6-1. Surveillance Capsule Geometry

TABLE 6-1

CALCULATED FAST NEUTRON EXPOSURE PARAMETERS AT THE CENTER OF CAPSULE P

	Cycle 1-13 [a]
ϕ (E> 1.0 MeV)[b]	7.66×10^{10}
ϕ (E> 0.1 MeV)[b]	2.74×10^{11}
dpa/sec	1.33×10^{-10}

(a) Averaged over the plant specific exposure for capsule P.

(b) n/cm^2 - sec

TABLE 6-2

CALCULATED FAST NEUTRON EXPOSURE PARAMETERS AT
THE PRESSURE VESSEL CLAD/BASE METAL INTERFACE

	AVERAGED OVER CYCLES 1-13			
	0°	15°	30°	45°
ϕ(E> 1.0Mev)[a]	3.76×10^{10}	2.35×10^{10}	1.75×10^{10}	1.58×10^{10}
ϕ(E> 0.1Mev)[a]	9.98×10^{10}	6.24×10^{10}	4.65×10^{10}	4.19×10^{10}
dpa/sec	6.22×10^{-11}	3.89×10^{-11}	2.90×10^{-11}	2.61×10^{-11}

(a) n/cm^2 - sec

TABLE 6-3

RELATIVE RADIAL DISTRIBUTIONS OF NEUTRON FLUX (E > 1.0 MeV) WITHIN THE PRESSURE VESSEL WALL

Radius (cm)	0°	15°	30°	45°
168.04(1)	1.00	1.00	1.00	1.00
168.71	0.935	0.938	0.936	0.937
170.12	0.816	0.817	0.814	0.818
171.53	0.680	0.689	0.683	0.691
172.94	0.563	0.573	0.566	0.574
174.35	0.462	0.473	0.465	0.473
175.75	0.376	0.388	0.380	0.388
177.16	0.305	0.316	0.309	0.316
178.57	0.246	0.256	0.250	0.256
179.98	0.196	0.206	0.201	0.206
181.39	0.155	0.164	0.160	0.164
182.80	0.118	0.128	0.125	0.129
183.83	0.0946	0.104	0.103	0.105
184.80(2)	0.0857	0.0967	0.0956	0.0982

NOTES: 1) Base Metal Inner Radius
2) Base Metal Outer Radius

TABLE 6-4

RELATIVE RADIAL DISTRIBUTIONS OF NEUTRON FLUX (E > 0.1 MeV)
WITHIN THE PRESSURE VESSEL WALL

Radius (cm)	0°	15°	30°	45°
168.04(1)	1.00	1.00	1.00	1.00
168.71	1.00	1.00	1.00	1.00
170.12	0.964	0.977	0.981	0.985
171.53	0.901	0.915	0.922	0.930
172.94	0.828	0.844	0.852	0.862
174.35	0.752	0.770	0.779	0.790
175.75	0.675	0.696	0.705	0.718
177.16	0.600	0.622	0.632	0.645
178.57	0.526	0.550	0.561	0.574
179.98	0.454	0.479	0.491	0.503
181.39	0.383	0.409	0.422	0.434
182.80	0.310	0.338	0.354	0.365
183.83	0.256	0.285	0.303	0.314
184.80(2)	0.234	0.267	0.287	0.298

NOTES: 1) Base Metal Inner Radius
2) Base Metal Outer Radius

TABLE 6-5

RELATIVE RADIAL DISTRIBUTIONS OF IRON DISPLACEMENT RATE (dpa) WITHIN THE PRESSURE VESSEL WALL

Radius (cm)	0°	15°	30°	45°
168.04(1)	1.00	1.00	1.00	1.00
168.71	0.944	0.947	0.945	0.946
170.12	0.832	0.833	0.830	0.834
171.53	0.714	0.723	0.717	0.726
172.94	0.625	0.636	0.628	0.637
174.35	0.545	0.558	0.549	0.558
175.75	0.466	0.481	0.471	0.481
177.16	0.400	0.414	0.405	0.414
178.57	0.344	0.358	0.350	0.358
179.98	0.290	0.305	0.297	0.305
181.39	0.243	0.257	0.251	0.257
182.80	0.196	0.212	0.208	0.214
183.83	0.163	0.179	0.177	0.181
184.80(2)	0.154	0.174	0.172	0.177

NOTES: 1) Base Metal Inner Radius
2) Base Metal Outer Radius

TABLE 6-6

NUCLEAR PARAMETERS FOR NEUTRON FLUX MONITORS

Monitor Material	Reaction of Interest	Target Weight Fraction	Response Range	Product Half-Life	
Copper	$Cu^{63}(n,\alpha)Co^{60}$	0.6917	$E > 4.7$ MeV	5.272 yrs	
Iron	$Fe^{54}(n,p)Mn^{54}$	0.058	$E > 1.0$ MeV	312.2 days	
Nickel	$Ni^{58}(n,p)Co^{58}$	0.6827	$E > 1.0$ MeV	70.91 days	
Uranium-238*	$U^{238}(n,f)Cs^{137}$	1.0	$E > 0.4$ MeV	30.17 yrs	6.0
Neptunium-237*	$Np^{237}(n,f)Cs^{137}$	1.0	$E > 0.8$ MeV	30.17 yrs	6.5
Cobalt-Aluminum*	$Co^{59}(n,\gamma)Co^{60}$	0.0015	$0.4 ev < E < 0.015$ MeV	5.272 yrs	
Cobalt-Aluminum	$Co^{59}(n,\gamma)Co^{60}$	0.0015	$E < 0.015$ MeV	5.272 yrs	

*Denotes that monitor is cadmium shielded.

TABLE 6-7

IRRADIATION HISTORY OF NEUTRON SENSORS CONTAINED IN CAPSULE P

Irradiation Period Month	Irradiation Period Year	P_j [a] (MW_t)	P_j [a] / $P_{Ref.}$	Irradiation Time (days)	Decay [b] Time (days)
4	1974	297.6	0.1804	17	5126
5	1974	807.0	0.4891	31	5095
6	1974	1201.3	0.7280	30	5065
7	1974	1044.2	0.6328	31	5034
8	1974	1575.4	0.9548	31	5003
9	1974	910.9	0.5520	30	4973
10	1974	426.9	0.2587	31	4942
11	1974	1044.7	0.6332	30	4912
12	1974	1220.0	0.7394	31	4881
1	1975	1050.9	0.6369	31	4850
2	1975	1381.4	0.8372	28	4822
3	1975	1474.4	0.8936	31	4791
4	1975	1149.2	0.6965	30	4761
5	1975	1175.4	0.7124	31	4730
6	1975	1080.3	0.6547	30	4700
7	1975	1132.2	0.6862	31	4669
8	1975	1580.1	0.9576	31	4638
9	1975	839.1	0.5086	30	4608
10	1975	1232.5	0.7470	31	4577
11	1975	1143.5	0.6930	30	4547
12	1975	1574.7	0.9544	31	4516
1	1976	1486.8	0.9011	31	4485
2	1976	720.7	0.4368	29	4456
3	1976	0.0	0.0000	31	4425
4	1976	523.7	0.3174	30	4395
5	1976	920.9	0.5581	31	4364
6	1976	474.4	0.2875	30	4334
7	1976	1587.0	0.9618	31	4303
8	1976	1600.8	0.9702	31	4272
9	1976	1473.4	0.8930	30	4242
10	1976	1611.4	0.9766	31	4211
11	1976	1591.5	0.9645	30	4181
12	1976	1595.6	0.9670	31	4150
1	1977	815.6	0.4943	31	4119
2	1977	0.0	0.0000	28	4091
3	1977	241.6	0.1464	31	4060
4	1977	1388.5	0.8415	30	4030
5	1977	1597.5	0.9682	31	3999
6	1977	1606.2	0.9734	30	3969
7	1977	1614.6	0.9786	31	3938
8	1977	1410.7	0.8550	31	3907
9	1977	1632.0	0.9891	30	3877
10	1977	1622.4	0.9832	31	3846
11	1977	1632.9	0.9896	30	3816
12	1977	1605.0	0.9727	31	3785

TABLE 6-7 (cont.)

IRRADIATION HISTORY OF NEUTRON SENSORS
CONTAINED IN CAPSULE P

Irradiation Period Month	Year	P_j[(a)] (MW_t)	P_j[(a)] / $P_{Ref.}$	Irradiation Time (days)	Decay[(b)] Time (days)
1	1978	1637.7	0.9926	31	3754
2	1978	1634.5	0.9906	28	3726
3	1978	1618.1	0.9807	31	3695
4	1978	1127.6	0.6834	30	3665
5	1978	97.4	0.0590	31	3634
6	1978	1412.3	0.8560	31	3604
7	1978	1518.6	0.9203	31	3573
8	1978	1590.0	0.9636	31	3542
9	1978	1579.2	0.9571	30	3512
10	1978	1623.8	0.9841	31	3481
11	1978	1568.6	0.9507	30	3451
12	1978	1613.7	0.9780	31	3420
1	1979	1629.1	0.9873	31	3389
2	1979	1558.9	0.9448	28	3361
3	1979	1526.5	0.9252	31	3330
4	1979	1599.4	0.9693	30	3300
5	1979	1316.4	0.7978	31	3269
6	1979	0.0	0.0000	30	3239
7	1979	0.0	0.0000	31	3208
8	1979	994.8	0.6029	31	3177
9	1979	1564.8	0.9483	30	3147
10	1979	1592.2	0.9650	31	3116
11	1979	1621.5	0.9827	30	3086
12	1979	1616.5	0.9797	31	3055
1	1980	958.5	0.5809	31	3024
2	1980	1616.1	0.9795	29	2995
3	1980	1643.9	0.9963	31	2964
4	1980	1632.6	0.9895	30	2934
5	1980	469.9	0.2848	31	2903
6	1980	191.6	0.1161	30	2873
7	1980	1595.2	0.9668	31	2842
8	1980	1512.6	0.9167	31	2811
9	1980	1314.4	0.7966	30	2781
10	1980	1587.5	0.9621	31	2750
11	1980	1644.4	0.9966	30	2720
12	1980	1597.4	0.9681	31	2689
1	1981	1644.4	0.9966	31	2658
2	1981	1604.1	0.9722	28	2630
3	1981	1528.1	0.9261	31	2599
4	1981	1079.4	0.6542	30	2569
5	1981	0.0	0.0000	31	2538
6	1981	1079.8	0.6544	30	2508
7	1981	1618.6	0.9810	31	2477
8	1981	1643.1	0.9958	31	2446
9	1981	1613.7	0.9780	30	2416

TABLE 6-7 (cont.)

IRRADIATION HISTORY OF NEUTRON SENSORS CONTAINED IN CAPSULE P

Irradiation Period Month	Year	P_j[a] (MW_t)	$\frac{P_j}{P_{Ref.}}$[a]	Irradiation Time (days)	Decay[b] Time (days)
10	1981	1573.6	0.9537	31	2385
11	1981	1594.7	0.9665	30	2355
12	1981	1638.8	0.9932	31	2324
1	1982	1617.6	0.9803	31	2293
2	1982	1600.0	0.9697	28	2265
3	1982	1646.0	0.9976	31	2234
4	1982	452.0	0.2744	30	2204
5	1982	280.4	0.1699	31	2173
6	1982	1615.8	0.9793	30	2143
7	1982	1637.3	0.9923	31	2112
8	1982	1643.0	0.9958	31	2081
9	1982	1639.9	0.9939	30	2051
10	1982	1632.8	0.9896	31	2020
11	1982	1636.5	0.9918	30	1990
12	1982	1448.2	0.8777	31	1959
1	1983	1637.7	0.9926	31	1928
2	1983	1641.0	0.9946	28	1900
3	1983	873.0	0.5291	31	1869
4	1983	0.0	0.0000	30	1839
5	1983	707.2	0.4286	31	1808
6	1983	1631.4	0.9887	30	1778
7	1983	1557.8	0.9441	31	1747
8	1983	1645.1	0.9970	31	1716
9	1983	1644.7	0.9968	30	1686
10	1983	1645.3	0.9971	31	1655
11	1983	1644.2	0.9965	30	1625
12	1983	1645.8	0.9975	31	1594
1	1984	1647.7	0.9986	31	1563
2	1984	1637.0	0.9921	29	1534
3	1984	716.3	0.4342	31	1503
4	1984	0.0	0.0000	30	1473
5	1984	1125.6	0.6822	31	1442
6	1984	1589.7	0.9635	30	1412
7	1984	1612.0	0.9770	31	1381
8	1984	1642.9	0.9957	31	1350
9	1984	1643.7	0.9962	30	1320
10	1984	1619.6	0.9816	31	1289
11	1984	1643.8	0.9962	30	1259
12	1984	1642.8	0.9956	31	1228
1	1985	1645.5	0.9973	31	1197
2	1985	403.3	0.2445	28	1169
3	1985	0.0	0.0000	31	1138
4	1985	948.2	0.5747	30	1108
5	1985	1629.6	0.9876	31	1077
6	1985	1638.2	0.9928	30	1047

TABLE 6-7 (cont.)

IRRADIATION HISTORY OF NEUTRON SENSORS CONTAINED IN CAPSULE P

Irradiation Period Month	Year	P_j [(a)] (MW_t)	$P_j / P_{Ref.}$ [(a)]	Irradiation Time (days)	Decay[(b)] Time (days)
7	1985	1638.1	0.9928	31	1016
8	1985	1543.7	0.9356	31	985
9	1985	1636.2	0.9916	30	955
10	1985	1643.8	0.9962	31	924
11	1985	1557.1	0.9437	30	894
12	1985	1587.8	0.9623	31	863
1	1986	1636.9	0.9921	31	832
2	1986	1587.8	0.9623	28	804
3	1986	0.0	0.0000	31	773
4	1986	372.1	0.2255	30	743
5	1986	1601.9	0.9709	31	712
6	1986	1634.6	0.9907	30	682
7	1986	1637.3	0.9923	31	651
8	1986	1585.8	0.9611	31	620
9	1986	1639.2	0.9934	30	590
10	1986	1615.7	0.9792	31	559
11	1986	1637.7	0.9925	30	529
12	1986	1634.2	0.9904	31	498
1	1987	1634.0	0.9903	31	467
2	1987	1376.0	0.8339	28	439
3	1987	0.0	0.0000	31	408
4	1987	1332.4	0.8075	30	378
5	1987	1593.9	0.9660	31	347
6	1987	1592.8	0.9653	30	317
7	1987	1591.0	0.9643	31	286
8	1987	1638.5	0.9930	31	255
9	1987	1622.3	0.9832	30	225
10	1987	1639.5	0.9936	31	194
11	1987	1634.7	0.9907	30	164
12	1987	1633.5	0.9900	31	133
1	1988	1636.5	0.9918	31	102
2	1988	1630.4	0.9881	29	73
3	1988	1205.9	0.7309	2	71

(a) P_j is average power in period j; P_{ref} is 1650 MW.

(b) Decay time is relative to the dosimetry counting reference date, 5/12/88.

TABLE 6-8

MEASURED [illegible]SOR ACTIVITIES AND REACTION RATES

Monitor and Axial Location	Measured Activity Bq/gm	Saturated Activity(a) Bq/gm	Reaction Rate (rps/nucleus
Cu-63 (n,α) Co-60			
Top-Middle	2.12×10^{5}	2.98×10^{5}	
Bottom-Middle	2.44×10^{5}	3.43×10^{5}	
Average	2.28×10^{5}	3.20×10^{5}	4.89×10^{-17}
Fe-54 (n,p) Mn-54			
Top	2.74×10^{6}	4.14×10^{6}	
Top-Middle	1.95×10^{6}	2.95×10^{6}	
Middle	2.11×10^{6}	3.19×10^{6}	
Bottom-Middle	2.19×10^{6}	3.31×10^{6}	
Bottom	2.33×10^{6}	3.52×10^{6}	
Average	2.26×10^{6}	3.42×10^{6}	5.45×10^{-15}
Ni-58 (n,p) Co-58			
Middle	2.44×10^{7}	4.83×10^{7}	6.89×10^{-15}

TABLE 6-8 (Cont'd)

MEASURED SENSOR ACTIVITIES AND REACTION RATES

Monitor and Axial Location	Measured Activity Bq/gm	Saturated Activity[(a)] Bq/gm	Reaction Rate (rps/nucleus)
Np-237 (n,f) Cs-137			
Middle	8.28×10^{6}	3.78×10^{7}	2.29×10^{-13}
U-238 (n,f) Cs-137			
Middle	1.13×10^{6}	5.16×10^{6}	3.41×10^{-14}
Co-59 (n,γ) Co-60			
Top	4.20×10^{7}	6.40×10^{7}	
Bottom	5.01×10^{7}	7.63×10^{7}	
Average	4.61×10^{7}	7.01×10^{7}	4.58×10^{-12}
Co-59 (n,γ) Co-60 (Cd)			
Top	1.79×10^{7}	2.73×10^{7}	
Bottom	2.04×10^{7}	3.11×10^{7}	
Average	1.92×10^{7}	2.92×10^{7}	1.92×10^{-12}

(a) Adjusted to center of surveillance capsule.

TABLE 6-9

SUMMARY OF NEUTRON DOSIMETRY RESULTS

	TIME AVERAGED EXPOSURE RATES	
ϕ (E > 1.0 MeV) {n/cm^2-sec}	8.27×10^{10}	$\pm$ 8%
ϕ (E > 0.1 MeV) {n/cm^2-sec}	2.87×10^{11}	$\pm$ 15%
dpa/sec	1.40×10^{-10}	$\pm$ 10%
ϕ(E < 0.414 eV) {n/cm^2-sec}	9.16×10^{10}	$\pm$ 19%
	INTEGRATED CAPSULE EXPOSURE	
ϕ (E > 1.0 MeV) {n/cm^2}	2.89×10^{19}	$\pm$ 8%
ϕ (E > 0.1 MeV) {n/cm^2}	1.00×10^{20}	$\pm$ 15%
dpa	4.90×10^{-2}	$\pm$ 10%
ϕ (E < 0.414 eV) {n/cm^2}	3.20×10^{19}	$\pm$ 19%

NOTE: Total Irradiation Time = 11.08 EFPY

TABLE 6-10

COMPARISON OF MEASURED AND FERRET CALCULATED
REACTION RATES AT THE SURVEILLANCE CAPSULE CENTER

Reaction	Measured	Adjusted Calculation	C/M
Cu-63 (n,α) Co-60	4.88×10^{-17}	5.03×10^{-17}	1.03
Fe-54 (n,p) Mn-54	5.45×10^{-15}	5.26×10^{-15}	0.96
Ni-58 (n,p) Co-58	6.89×10^{-15}	6.92×10^{-15}	1.01
U-238 (n,f) Cs-137 (Cd)	2.69×10^{-14}	2.71×10^{-14}	1.01
Np-237 (n,f) Cs-137 (Cd)	2.29×10^{-13}	2.32×10^{-13}	1.01
Co-59 (n,γ) Co-60	4.44×10^{-12}	4.44×10^{-12}	1.00
Co-59 (n,γ) Co-60 (Cd)	1.85×10^{-12}	1.85×10^{-13}	1.00

TABLE 6-11
ADJUSTED NEUTRON ENERGY SPECTRUM AT THE SURVEILLANCE CAPSULE CENTER

Group	Energy (MeV)	Adjusted Flux (n/cm^2-sec)	Group	Energy (MeV)	Adjusted Flux (n/cm^2-sec)
1	1.733E+01	6.87E+06	28	9.119E-03	1.17E+10
2	1.492E+01	1.55E+07	29	5.531E-03	1.42E+10
3	1.350E+01	6.00E+07	30	3.355E-03	4.44E+09
4	1.162E+01	1.36E+08	31	2.839E-03	4.22E+09
5	1.000E+01	3.04E+08	32	2.404E-03	4.10E+09
6	8.607E+00	5.34E+08	33	2.035E-03	1.20E+10
7	7.408E+00	1.27E+09	34	1.234E-03	1.20E+10
8	6.065E+00	1.89E+09	35	7.485E-04	1.19E+10
9	4.966E+00	4.00E+09	36	4.540E-04	1.18E+10
10	3.679E+00	5.15E+09	37	2.754E-04	1.24E+10
11	2.865E+00	1.03E+10	38	1.670E-04	1.40E+10
12	2.231E+00	1.32E+10	39	1.013E-04	1.29E+10
13	1.738E+00	1.74E+10	40	6.144E-05	1.27E+10
14	1.353E+00	1.79E+10	41	3.727E-05	1.23E+10
15	1.108E+00	3.11E+10	42	2.260E-05	1.18E+10
16	8.208E-01	3.2[illegible]E+10	43	1.371E-05	1.14E+10
17	6.393E-01	3.21E+10	44	8.315E-06	1.09E+10
18	4.979E-01	2.24E+10	45	5.043E-06	1.02E+10
19	3.877E-01	2.94E+10	46	3.059E-06	9.69E+09
20	3.020E-01	3.26E+10	47	1.855E-06	9.07E+09
21	1.832E-01	2.99E+10	48	1.125E-06	7.63E+09
22	1.111E-01	2.36E+10	49	6.826E-07	7.68E+09
23	6.738E-02	1.73E+10	50	4.140E-07	1.23E+10
24	4.087E-02	1.08E+10	51	2.511E-07	1.26E+10
25	2.554E-02	1.16E+10	52	1.523E-07	1.28E+10
26	1.989E-02	7.30E+09	53	9.237E-08	5.40E+10
27	1.503E-02	1.00E+10			

NOTE: Tabulated energy levels represent the upper energy of each group.

TABLE 6-12

COMPARISON OF CALCULATED AND MEASURED
EXPOSURE LEVELS FOR CAPSULE P

	Calculated	Measured	C/M
$\phi(E > 1.0\ MeV)\ (n/cm^2)$	2.68×10^{19}	2.89×10^{19}	0.93
$\phi(E > 0.1\ MeV)\ (n/cm^2)$	9.60×10^{19}	1.00×10^{20}	0.96
dpa	4.67×10^{-2}	4.90×10^{-2}	0.95
$\phi(E < 0.414\ eV)\ (n/cm^2)$	2.87×10^{19}	3.20×10^{19}	0.90

TABLE 6-13

NEUTRON EXPOSURE PROJECTIONS AT LOCATIONS

ON THE PRESSURE VESSEL CLAD/BASE METAL INTERFACE

	AZIMUTHAL ANGLE			
	0°[a]	15°	30°	45°
11.08 EFPY				
Φ (E> 1.0 MeV)(b)	1.42×10^{19}	8.87×10^{18}	6.60×10^{18}	5.96×10^{18}
Φ (E> 0.1 MeV)(b)	3.77×10^{19}	2.36×10^{19}	1.75×10^{19}	1.58×10^{19}
dpa	2.35×10^{-2}	1.47×10^{-2}	1.09×10^{-2}	9.87×10^{-3}
32.0 EFPY				
Φ (E> 1.0 MeV)(b)	3.90×10^{19}	2.44×10^{19}	1.82×10^{19}	1.64×10^{19}
Φ (E> 0.1 MeV)(b)	1.04×10^{20}	6.48×10^{19}	4.83×10^{19}	4.36×10^{19}
dpa	6.46×10^{-2}	4.04×10^{-2}	3.01×10^{-2}	2.72×10^{-2}

(a) Maximum point on the pressure vessel

(b) n/cm^2

TABLE 6-14

VESSEL NEUTRON EXPOSURE VALUES (E>1.0 MeV) FOR USE IN THE GENERATION OF HEATUP/COOLDOWN CURVES

20 EFPY

	NEUTRON FLUENCE (E> 1.0 MeV) SLOPE (n/cm^2)			dpa SLOPE (n/cm^2)		
	Surface	1/4 T	3/4 T	Surface	1/4 T	3/4 T
0°(a)	2.48×10^{19}	1.54×10^{19}	4.41×10^{18}	2.48×10^{19}	1.66×10^{19}	6.67×10^{18}
15°	1.55×10^{19}	9.78×10^{18}	2.90×10^{18}	1.55×10^{19}	1.05×10^{19}	4.40×10^{18}
30°	1.15×10^{19}	7.19×10^{18}	2.10×10^{18}	1.15×10^{19}	7.74×10^{18}	3.17×10^{18}
45°	1.04×10^{19}	6.58×10^{18}	1.94×10^{18}	1.04×10^{19}	7.09×10^{18}	2.95×10^{18}

32 EFPY

	NEUTRON FLUENCE (E> 1.0 MeV) SLOPE (n/cm^2)			dpa SLOPE (n/cm^2)		
	Surface	1/4 T	3/4 T	Surface	1/4 T	3/4 T
0°(a)	3.90×10^{19}	2.43×10^{19}	6.94×10^{18}	3.90×10^{19}	2.61×10^{19}	1.05×10^{19}
15°	2.44×10^{19}	1.54×10^{19}	4.56×10^{18}	2.44×10^{19}	1.66×10^{19}	6.93×10^{18}
30°	1.82×10^{19}	1.14×10^{19}	3.33×10^{18}	1.82×10^{19}	1.22×10^{19}	5.02×10^{18}
45°	1.64×10^{19}	1.04×10^{19}	3.07×10^{18}	1.64×10^{19}	1.12×10^{19}	4.66×10^{18}

(a) Maximum point on the pressure vessel

TABLE 6-15

UPDATED LEAD FACTORS FOR KEWAUNEE SURVEILLANCE CAPSULES

Capsule	Lead Factor
V	Removed (1.29 EFPY)
R	Removed (4.57 EFPY)
P	Removed (11.08 EFPY)
T	2.04
S	1.91
N	1.91

SECTION 7
SURVEILLANCE CAPSULE REMOVAL SCHEDULE

The following removal schedule meets ASTM E185-82 and is recommended for future capsules to be removed from the Kewaunee reactor vessel:

Capsule	Vessel Location (deg)	Lead Factor	Removal Time(a)	Estimated Capsule Fluence (n/cm^2)
V	77	-	1.29	5.99×10^{18}(b)
R	257	-	4.57	2.07×10^{19}(b)
P	247	-	11.08	2.89×10^{19}(b)
T	67	2.04	16	4.00×10^{19}(c)
S	57	1.91	32	7.45×10^{19}
N	237	1.91	Standby	--

a) Effective full power years from plant startup

b) Actual fluence

c) Approximate fluence at vessel inner wall at end of design life (32 EFPY)

SECTION 8
REFERENCES

1. Yanichko, S. E. et. al., "Wisconsin Public Service Corp. Kewaunee Nuclear Power Plant Reactor Vessel Radiation Surveillance Program, WCAP-8107, April 1973.

2. Yanichko, S. E. et. al. "Analysis of Capsule V from the Wisconsin Public Service Corporation Kewaunee Nuclear Plant Reactor Vessel Radiation Surveillance Program," WCAP-8908, January 1977.

3. Yanichko, S. E., et. al. "Analysis of Capsule R from the Wisconsin Public Service Corporation Kewaunee Nuclear Plant Reactor Vessel Radiation Surveillance Program," WCAP-9878, March 1981.

4. Code of Federal Regulations, 10CFR50, Appendix G, "Fracture Toughness Requirements" and Appendix H, "Reactor Vessel Material Surveillance Program Requirements," U.S. Nuclear Regulatory Commission, Washington, DC.

5. Regulatory Guide 1.99, Revision 2, "Radiation Embrittlement of Reactor Vessel Materials," U.S. Nuclear Regulatory Commission, May, 1988.

6. ASTM Designation E693-79, "Standard Practice for Characterizing Neutron Exposures in Ferritic Steels in Terms of Displacements per Atom (dpa)", in ASTM Standards, Section 12, American Society for Testing and Materials, Philadelphia, PA, 1984.

7. R. G. Soltesz, R. K. Disney, J. Jedruch, and S. L. Ziegler, "Nuclear Rocket Shielding Methods, Modification, Updating and Input Data Preparation. Vol. 5--Two-Dimensional Discrete Ordinates Transport Technique", WANL-PR(LL)-034, Vol. 5, August 1970.

8. "ORNL RSIC Data Library Collection DLC-76, SAILOR Coupled Self-Shielded, 47 Neutron, 20 Gamma-Ray, P3, Cross Section Library for Light Water Reactors".

9. ASTM Designation E482-82, "Standard Guide for Application of Neutron Transport Methods for Reactor Vessel Surveillance", in ASTM Standards, Section 12, American Society for Testing and Materials, Philadelphia, PA, 1984.

10. ASTM Designation E560-77, "Standard Recommended Practice for Extrapolating Reactor Vessel Surveillance Dosimetry Results", in ASTM Standards, Section 12, American Society for Testing and Materials, Philadelphia, PA, 1984.

11. ASTM Designation E706-81a, "Standard Master Matrix for Light-Water Reactor Pressure Vessel Surveillance Standard", in ASTM Standards, Section 12, American Society for Testing and Materials, Philadelphia, PA, 1984.

12. ASTM Designation E853-84, "Standard Practice for Analysis and Interpretation of Light-Water Reactor Surveillance Results", in ASTM Standards, Section 12, American Society for Testing and Materials, Philadelphia, PA, 1984.

13. ASTM Designation E261-77, "Standard Method for Determining Neutron Flux, Fluence, and Spectra by Radioactivation Techniques", in ASTM Standards, Section 12, American Society for Testing and Materials, Philadelphia, PA, 1984.

14. ASTM Designation E262-77, "Standard Method for Measuring Thermal Neutron Flux by Radioactivation Techniques", in ASTM Standards, Section 12, American Society for Testing and Materials, Philadelphia, PA, 1984.

15. ASTM Designation E263-82, "Standard Method for Determining Fast-Neutron Flux Density by Radioactivation of Iron", in ASTM Standards, Section 12, American Society for Testing and Materials, Philadelphia, PA, 1984.

16. ASTM Designation E264-82, "Standard Method for Determining Fast-Neutron Flux Density by Radioactivation of Nickel", in ASTM Standards, Section 12, American Society for Testing and Materials, Philadelphia, PA, 1984.

17. ASTM Designation E481-78, "Standard Method for Measuring Neutron-Flux Density by Radioactivation of Cobalt and Silver", in ASTM Standards, Section 12, American Society for Testing and Materials, Philadelphia, PA, 1984.

18. ASTM Designation E523-82, "Standard Method for Determining Fast-Neutron Flux Density by Radioactivation of Copper", in ASTM Standards, Section 12, American Society for Testing and Materials, Philadelphia, PA, 1984.

19. ASTM Designation E704-84, "Standard Method for Measuring Reaction Rates by Radioactivation of Uranium-238", in ASTM Standards, Section 12, American Society for Testing and Materials, Philadelphia, PA, 1984.

20. ASTM Designation E705-79, "Standard Method for Measuring Fast-Neutron Flux Density by Radioactivation of Neptunium-237", in ASTM Standards, Section 12, American Society for Testing and Materials, Philadelphia, PA, 1984.

21. ASTM Designation E1005-84, "Standard Method for Application and Analysis of Radiometric Monitors for Reactor Vessel Surveillance", in ASTM Standards, Section 12, American Society for Testing and Materials, Philadelphia, PA, 1984.

22. F. A. Schmittroth, FERRET Data Analysis Code, HEDL-TME 79-40, Hanford Engineering Development Laboratory, Richland, WA, September 1979.

23. W. N. McElroy, S. Berg and T. Crocket, A Computer-Automated Iterative Method of Neutron Flux Spectra Determined by Foil Activation, AFWL-TR-67-41, Vol. I-IV, Air Force Weapons Laboratory, Kirkland AFB, NM, July 1967.

24. EPRI-NP-2188, "Development and Demonstration of an Advanced Methodology for LWR Dosimetry Applications", R. E. Maerker, et al., 1981.